

Dear Editors,

On behalf of my co-authors, we thank you very much for giving us an opportunity to revise our manuscript, and we also appreciate reviewers very much for their positive and constructive comments and suggestions on our manuscript entitled “*Holocene vegetation dynamics in response to climate change and hydrological processes in the Bohai region*” (Manuscript Number: cp-2020-20).

We have studied reviewers’ comments carefully and have revised our manuscript. Attached please find the revised version and relevant document, which we would like to submit for your kind consideration.

Once again, thank you very much for your comments and suggestions. And we hope that the corrections will meet with approval. If you have any questions, please don’t hesitate to contact me at the address below.

Thank you and best regards.

Yours sincerely,

Chen Jinxia and Shi Xuefa

Corresponding authors:

Chen Jinxia, E-mail: jinxiachen@fio.org.cn

Key Laboratory of Marine Geology and Metallogeny, MNR, Qingdao 266061, China

Shi Xuefa, E-mail: xfshi@fio.org.cn

Key Laboratory of Marine Geology and Metallogeny, MNR, Qingdao 266061, China

Dear editor and kind reviewers,

We've revised our MS following all the very helpful comments and excellent suggestions to improve the paper technically and linguistically, and the point by point updates and explanations are listed below:

Referee #1:

This manuscript (MS) by Jinxia et al. describes the results of a palynological and sedimentological study based on a core taken from the Laizhou Bay in the Bohai Sea, eastern China. The MS is generally well written (some remarks concerning grammar etc. and also concerning redundancies are mentioned later), and I think the results are worth being presented since they are at least of regional importance. I am not completely sure though if the results are completely fitting with the scope of *Climate of the Past*. I have marked the scientific significance as 'good', but in the current stage it is rather between good and fair - if additional methods were used to generate climate data via the described record and if certain aspects would be discussed in more detail, 'good' would probably be fitting.

I must admit in this context that I am not familiar with the research region. It seems some of the authors have also contributed to additional studies from the Bohai region, and I was concerned that there might be some redundancy to these different studies. It seems though that a medium- to high resolution study comprising the Holocene has not yet been published for the region, and the earlier studies are incorporated into the discussion.

*Thank you for the comments and constructive suggestions for improving our MS. We've thoroughly revised this MS following your helpful comments. Thanks again for giving this paper a golden chance to be reconsidered for publication in *Climate of the Past*.*

Question 1.

Several palynological aspects are well incorporated into the manuscript, but a potential degradation of pollen grains is not appropriately discussed in my opinion. The

authors correctly refer to the possible problem that there may be a transportation bias concerning bisaccate pollen (it should be considered that this may also affect Poaceae and perhaps Cyperaceae values). They also mention that the suspension of pollen grains may play an important role. But pollen concentration varies between less than 100 grains/g (which is quite low!) and several thousand grains/g in this record – this may also point to a degradation signal. Just for example, note that *Pinus* pollen, which is probably much more resistant to degradation than certain nonsaccate pollen such as *Quercus* or *Chenopodiaceae* (compare e.g. Cheddai & Rossignol-Strick 1995 or Havinga 1967), increases relatively in those sections of the core which are characterized by higher sand content (and thus probably are better oxygenated). I think the aspect of pollen preservation should be mentioned in detail at the onset of the discussion and considered throughout.

Answer:

We thank the referee for this constructive comment. We totally agree with this comment that pollen preservation should be considered in discussion because the composition of a fossil pollen in sediment depends on several different factors including the composition of the vegetation from which the pollen originates, pollen dispersion, deposition and preservation. In a dynamic environment such as the Bohai coastal area, bias originated from bad preservation should be eliminated before using the net content of pollen grains to reconstruct paleovegetation.

In this study, the pollen concentration ranged from 62 to 6050 grains/g. Relatively low pollen concentrations were found in the two sections (160–135 cm and 34–19 cm), largely correlated to high sand contents as revealed by the lithology. Especially for the lower section (150–135 cm), the high portion of sand content is consistent with a low pollen concentration and a high percentage of *Pinus* pollen. As the *Pinus* is more resistant to degradation, the variations of total pollen concentration as well as higher percentage of *Pinus* in this section seem to be related to pollen preservation.

However, as revealed by figure 1, the highest percentage of *Pinus* recorded in depth of 150–128 cm, with a minor value at 145–143 cm, which is not completely in conformity with the high sand content section in the same core (160–135 cm). Similarly,

for the upper section, high sand content was recorded in depth of 34-19 cm. However, the percentage of *Pinus* is low in this section except a relative high value in depth of 21 cm (figure 1). We thus suggest degradation is not a key point influencing the concentration of pollen and spore in the studied area. Alternatively, regional hydrodynamic conditions may be the dominated factor for the deposition of pollen and spore.

Previous research suggests that the sedimentation mechanisms of pollen and spore in marine water is similar to that of sediment with clay- and fine silt- grain size (Heusser, 1988). After transported to the Bohai Sea, the pollen and spore may deposit with sediment and follows the grain size control principle. A recent investigation on the surface sediment from the Bohai Sea shows high pollen concentration in fine sediments such as clay and silty clay while low pollen concentration in coarse sediment with high percentage of sand content (figure 2; Yang et al., 2019). Yang et al. (2019) attributed the low pollen concentration in areas with a high sand content of the Bohai Sea could be attributed to the strong hydrodynamic suspension and screening for sediments and pollen.

Therefore, we conclude that the low pollen concentrations in the two sections (160-135 cm, and 34-19 cm), correlated with high sand content, could be contribute to hydrodynamic condition rather than degradation.

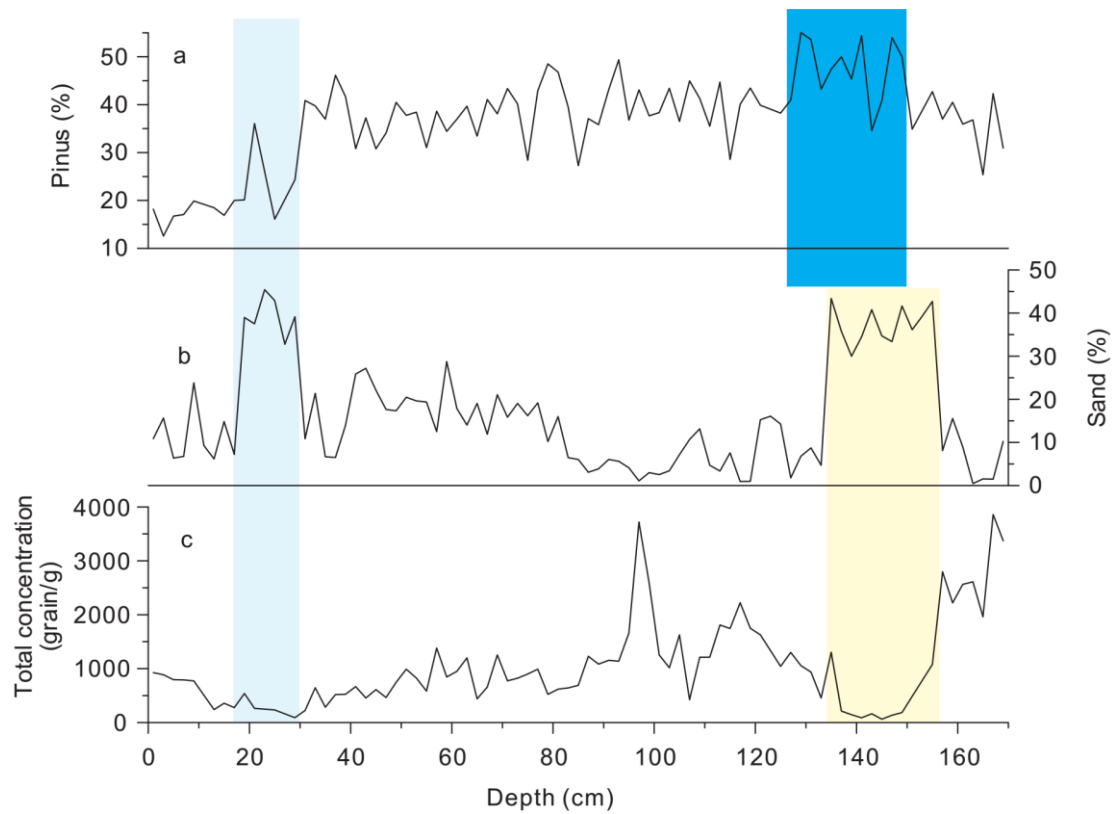


Figure 1: Comparison of *Pinus* percentage (a), sand percentage (b) and palynomorph concentration (c) in core CJ06-435 at the depth of 0-170 cm.

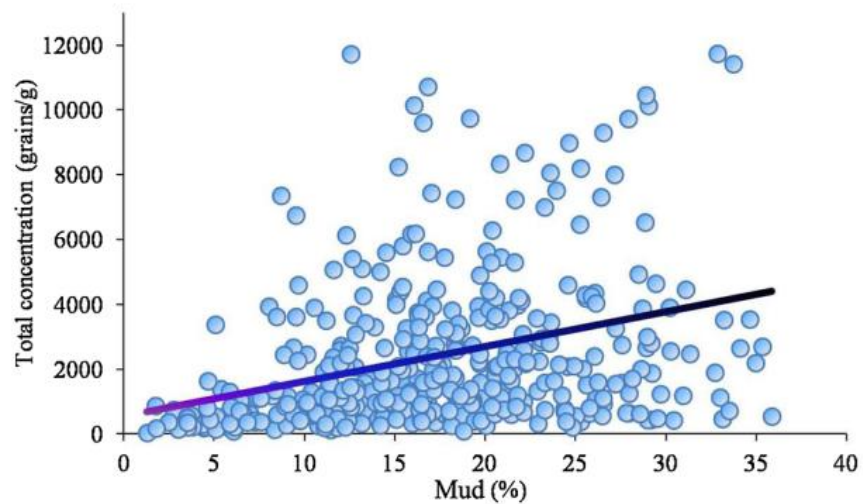


Figure 2: The relationship between the total pollen concentration and mud content (%) in surface sediments of Bohai Sea, it showed that high pollen concentration were closely correlated with fine-sized sediment (Yang et al., 2019).

Heusser, L.E., 1988. Pollen distribution in marine sediments on the continental margin off northern California. *Mar. Geol.* 80, 131–147.

Yang, S.X., Song, B., Ye, S.Y., Laws, E.A., He, L., Li, J., Chen, J.X., Zhao, G.M., Zhao, J.T., Mei, X., Behling, H., 2019. Large-scale pollen distribution in marine surface sediments from the Bohai Sea, China: Insights into pollen provenance, transport, deposition, and coastal-shelf paleoenvironment. *Progress in Oceanography*. 178, 102183.

Question 2.

Another weakness is the age model, particularly in the upper part of the core. The authors dismiss three foraminifer-based ages in favor of one Cs age in the upper section of the core, which may be okay – but then it should be discussed in detail what may have caused that these ages are ca. 3000 yr too old, and how the reader can be sure that the other foraminifer-based ages are correct. It should be mentioned, considering the problems with the uppermost ages, which foraminifer species were chosen (probably benthics?). If the used ages are correct, the 35-cm-section between 25 and 60 cm comprises more than 3000 yr, but the lower 120 cm comprise also ca. 3000 yr. This is certainly tied to the sedimentological aspects which are discussed (particularly the shift(s) of the the Yellow River Channel) by the authors, but in my opinion there remain a lot of uncertainties concerning the ages particularly above 60 cm depth. Therefore, it seems problematic to me to mention quite precise ages for the uppermost 60 cm (as done e.g. in the abstract, see below). Consider also a possible problem in Tab. 1 (see below). And how have you dealt with the older age at 119 cm compared to the younger at 129 cm – could it be redeposition? Was one age excluded?

Answer:

We thank the referee for this tough but constructive comment. Actually, the age model was a critical question for us, since we have tested lots of AMS¹⁴C dating points. But some of the results are confused. And, the part of age model was weak in the original MS. We rewrote the age model part in the revised manuscript and gave a detailed discussion for the current age model. Some major points are listed as follow.

(1) Indeed, neither of the single species of foraminifera is enough for AMS¹⁴C dating in our core. We had to mixed all kinds of benthic foraminifera for dating (Detailed introduce was added in the revised Table 1).

(2) We eliminated the dating point of 129 cm because we believed that it appears not to be reliable. According to He et al. (2019) result, the calculated sedimentation rate (CSR) in the tidal flat and neritic area of the south Bohai Sea ranged in 0.02-0.13 cm/year before ca. 2000 cal. a BP (by interpolation dating and calculation from cores H9601, H9602, ZK228, and ZK1, Figure 3). Therefore if the 129 cm dating is correct, the CSR would be as high as 0.45 cm/yr in the section of 87-129 cm (4801-4894 cal. a BP). It is apparently not reasonable because core CJ06-435 is off-shore compared to those cores (e.g. H9601, H9602, ZK228, and ZK1, Figure 3) reported in He et al. (2019) research. Thus it should have lower CSR than those cores rather than a approximate tenfold increase in CSR.

(3) Based on the original age model, the record between 3000 cal. a BP and 1855 AD is somewhat confused. Because the CSR was extremely low during 3000 a BP-1855 AD (about 0.005 cm/yr). As reported in the recent study, cores from the tidal flat and neritic sea of the south Bohai Sea recorded CSR ranged in 0.02-0.13 cm/yr before 2000 cal. a BP (apparent in cores H9601, H9602, ZK228, and ZK1, Figure 3; He et al., 2019), 0.04-0.06 cm/yr between 2000 cal. a BP to 1855 AD (apparent in core ZK228, HB-1 and GYDY, Figure 3; He et al., 2019), and 0.35-1.38 cm/yr since 1855 AD (Wu et al., 2015; Qiao et al., 2017; Xu et al., 2018). Therefore, we also suggest that the primary age model covered the period of 3000 a BP-1855 AD is open to question. We guess there might be some deposition hiatus between 3000 cal. a BP and 1855 AD. Beyond that our age model and the calculated CSR in the upper unit (since 1855 AD, as calculated to 0.17-0.48 cm/yr) and the lower unit (3000-8500 cal. a BP, as calculated to 0.016-0.057 cm/yr) are comparable to the nearby records by He et al. (2019) and Xu et al. (2018).

As a response, we just focused on the climate change between 3000-8500 a BP and only gave a cautious discussion for the chronology uncertain interval in the revised manuscript.

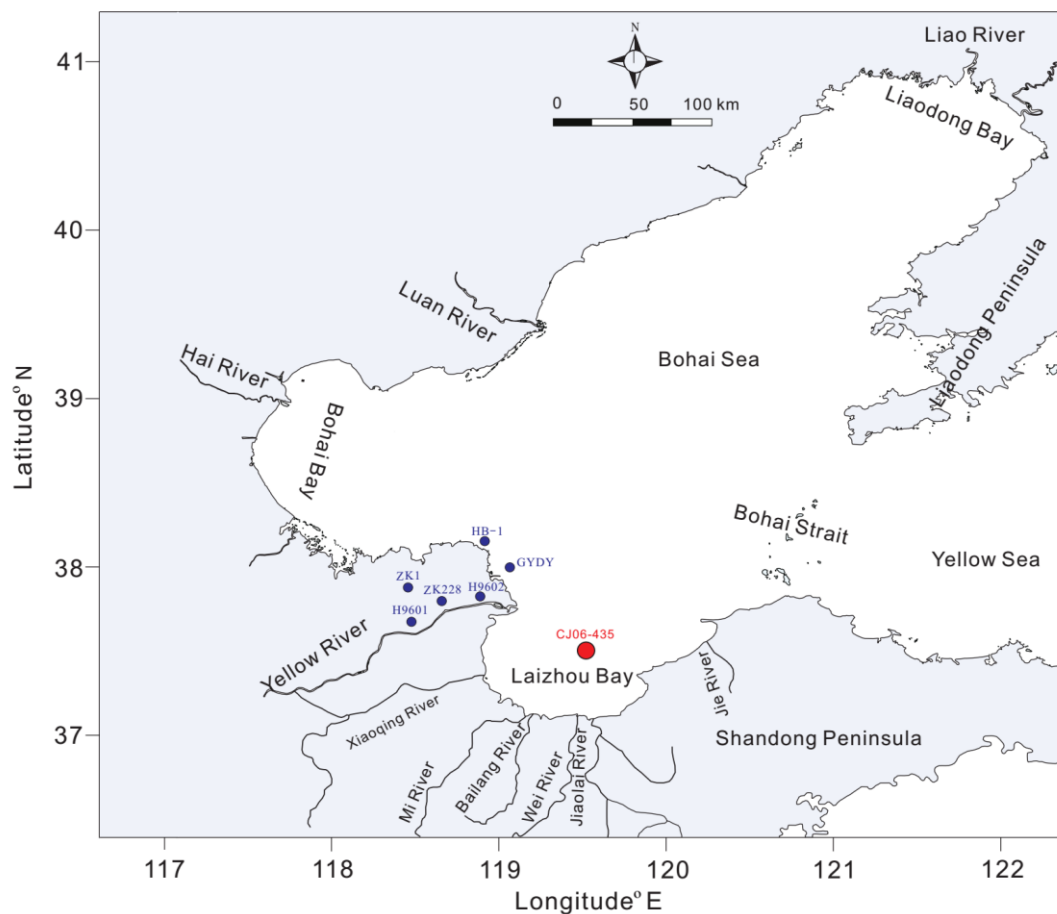


Figure 3: Locations of core CJ06-435 and other nearby cores.

He, L., Xue, C.T., Ye, S.Y., Amorosi, A., Yuan, H.M., Yang, S.X., Laws, E.A.: New evidence on the spatial-temporal distribution of superlobes in the Yellow River Delta Complex, *Quat. Sci. Rev.*, 214, 117–138, 2019.

Qiao, S.Q., Shi, X.F., Wang, G.Q., Zhou, L., Hu, B.Q., Hu, L.M., Yang, G., Liu, Y.G., Yao, Z.Q., Liu, S.F.: Sediment accumulation and budget in the Bohai Sea, Yellow Sea and East China Sea. *Mar. Geol.*, 390, 270-281, 2017.

Wu, X., Bi, N.S., Kanai, Y., Saito, Y., Zhang, Y., Yang, Z.S., Fan, D.J., Wang, H.J.: Sedimentary records off the modern Huanghe (Yellow River) delta and their response to deltaic river channel shifts over the last 200 years, *J. Asian Earth Sci.*, 108, 68–80, 2015.

Xu, Y.P., Zhou, S.Z., Hu, L.M., Wang, Y.H., Xiao, W.J.: Different controls on sedimentary organic carbon in the Bohai Sea: River mouth relocation, turbidity and eutrophication. *J. Marine. Syst.*, 180, 1-8, 2018.

Question 3.

I cannot say much about the sedimentological interpretation. Concerning the

198 palynology-related sections of the interpretation, I think they are quite well written
199 (though the preservation and age model ‘problems’ should be considered more often,
200 particularly when it comes to the interpretation of stages 2c to 3). I wondered in this
201 context if the results of Li et al. 2019 would be worth being mentioned here since the
202 record presented in the MS seems to cover the end of the Holocene climatic optimum.

203 **Answer:**

204 Thanks for this good advice and the valuable literature recommends. In the revised
205 manuscript Section 5.4 , we elaborately discussed our finding referring to other reported
206 findings in north China (such as Ren and Zhang, 1998; Yi et al., 2003; Chen et al., 2012;
207 Stebich et al., 2015; Sun and Feng, 2015; Hao et al., 2016; Li et al., 2019; Li et al., 2020;
208 etc.) for a better interpreting of paleovegetation and paleoclimate evolution.

209
210 **Question 4.**

211 What concerns me particularly when it comes to the relevance of this MS for Climate
212 of the past is section 5.5, in which the authors link their own data to other climate
213 records. A) Since the authors show their own data vs age (Fig. 8), it should be clearly
214 stated how the age model was composed (linear interpolation?), it is not enough to show
215 the dates in Tab. 1. What a about the ages at 119 and 129 cm?

216 **Answer:**

217 We are sorry for this mistake. Indeed this was an incorrect writing in Tabal.1. We have
218 corrected this mistake in the revised manuscript.

219 The age model was established by assuming constant sedimentation rates between two
220 contiguous control points and extrapolation after the oldest control point.

221
222 **Question 5.**

223 B) Quercus, as the authors explain, has several species in the region, therefore, the
224 climatic susceptibility of this genus might be relatively low, and several factors, not
225 only temperature, are influencing its relative occurrences in the pollen record. Quercus
226 pollen is also quite susceptible to taphonomical bias (s.a.). For example, the Quercus
227 curve of the Feng et al. (2017) record the authors cite is (naturally) completely different.

C) Two other studies with pollen-based climate reconstructions which are included in Fig. 8 work with quantitative reconstructions – if the authors want their own data to be directly comparable, they should also use such an approach. The whole section 5.5 seems a little bit like an addition to make the paper a ‘climate paper’. This is also consistent with some inconsistencies concerning the related Fig.8 (see below). In order to make this MS appropriate for Climate of the Past, I would suggest to use the pollen data as base for quantitative climate data. The results should be incorporated in the climate-related section. The other aspects I mentioned (taphonomy/degradation and discussion of the age model/interpolation) should be considered, too, and discussed appropriately.

Answer:

The authors are grateful for this constructive comment. The referee gave several useful advices which we believe can promote this study.

(1) Fossil pollen spectra preserved in terrestrial sediments has been employed as a robust proxy for quantitative climate reconstructions in many regions of the world. However, quantitative palaeoclimatological estimates by marine sediments pollen data is very rare. It is probably because the quantitative reconstruction results from marine pollen data are not ideal. In the revised manuscript, we tried to use pollen data of core CJ06-435 as base for quantitative climate reconstruction. The reconstructed annual mean temperature (TANN) values ranges from 3.7°C to 6.9 °C for the past 8500 cal. a BP. However, the reconstructed TANN is much lower than the modern average annual temperature around Laizhou Bay (~12.5 °C). Therefore, we consider that the quantitative estimates results by pollen data of core CJ06-435 (a marine sediment core) may not be satisfactory.

(2) *Quercus* has many species in the world. Different response of *Quercus* growth to climate in different region. *Quercus* mainly composed of *Q. acutissima*, *Q. mongolica*, and *Q. liaotungensis* in the land areas surrounding the Bohai Sea. Among these, *Q. acutissima* and *Pinus densiflora* forests develop in the low mountains and hilly area of Shandong Peninsula. *Q. mongolica*, *Q. acutissima* and *P. densiflora* develop in the Liaodong Peninsula (Li et al., 2007; Xu et al., 2010).

It's worth noting that the pollen assemblages in marine surface sediments from the Laizhou Bay revealed that higher concentrations of *Quercus* and *Pinus* pollen distributed in the east of Laizhou Bay, and lower concentrations in the nearshore area outside the estuary of the Yellow River (Figure 4a and b). The distribution of *Quercus* and *Pinus* pollen concentration in surface sediment shows a clearly increasing shoreward the Shandong Peninsula and it is a good indicator for source tracing. In the low mountains and hilly area of Shandong Peninsula, the vegetation is characterized chiefly by *Q. acutissima* and *P. densiflora* forests. Modern research found that incremental temperature had positive impacts on radial growth of *Q. acutissima* and negative impacts on that of *P. densiflora* (Byun et al., 2013). For example, with the rise of annual mean temperature, *Q. acutissima* forests have naturally increased by approximately 1.13% in South Korea from 1996 to 2010, while *P. densiflora* decreased by 4% (Korea Forest Service, 2011; Kim et al., 2011). Therefore, the variations of *Quercus* and *Pinus* pollen from Shandong Peninsula may be related to temperature change.

Except Shandong Peninsula, pollen from other regions around Laizhou Bay (such as Liaodong Peninsula) may also be transported to the Laizhou Bay, and deposited in core CJ06-435.

Previous studies revealed that *Quercus* and *Pinus* were the dominant components of the forests in northeast China (including the land areas surrounding the Bohai Sea) during the Holocene. The variation of *Quercus* and *Pinus* contents were closely related to the change of temperature (Ren and Zhang, 1998; Li et al., 2004; Xu et al., 2014; Zhang et al., 2019). Ren and Zhang (1998) investigated pollen data from Northeast China and found that *Quercus* and *Ulmus* were the dominant components of the forests in northeast China between 10 and 5 ka, while *Pinus* were much more sparse, indicating a warmer and drier summers in northeast China for the early to mid-Holocene. A high-resolution 1000-year pollen record from the Sanjiaowan Marr Lake (42° 22' 16" N, 126° 25' 39" E) in northeastern China revealed that *Quercus* is a effective indicator for temperature reconstructing. Several notable cold periods, with lower *Quercus* frequencies, occurred at approximately 1200 AD, 1410 AD, 1580 AD, 1770 AD and

1870 AD (Zhang et al., 2019). Another 5350-year pollen record from an annually laminated maar lake (42 °18.0' N, 126 °21.5' E) revealed a decrease of *Quercus* and an increases of *Pinus* component, indicated a cooling trend during the past 5350 years (Xu et al., 2014).

So, we suggested that *Quercus* is a suitable pollen type for indicating temperature variations in our study region.

(3) As inferred by **Referee #1** and **Referee #2**, Section 5.4 “Palaeovegetation reconstruction and its climate significance” and Section 5.5 “Holocene temperature variations in North China and possible driving mechanisms” need more detailed discussion.

We rewrote this part in the revised manuscript. We calculated the ratio of *Quercus* to *Pinus* pollen (Q/P). Referring to previous studies such as Ren and Zhang (1998), Xu et al. (2014) and Zhang et al. (2019), the ratios of Q/P and *Quercus* percentage of core CJ06-435 were chosen to indicate regional temperature change, with high values indicating warm conditions. More detailed comparison of our results with global and regional climate records (we added some marine temperature records, such as Jia et al. (2019)) were presented in **Section 5.5** of the revised manuscript.

In **Section 5.4**, we gave a more detailed discussion of pollen percentage and concentration, the ecology and spread characteristics of main pollen species in core CJ06-435, paleovegetation and paleoclimate evolution of the study region and correlation and teleconnection with other findings in north China (such as Ren and Zhang, 1998; Yi et al., 2003; Chen et al., 2012; Stebich et al., 2015; Sun and Feng, 2015; Hao et al., 2016; Li et al., 2019; Li et al., 2020; etc.). We hope the revised part will be more logical and readable.

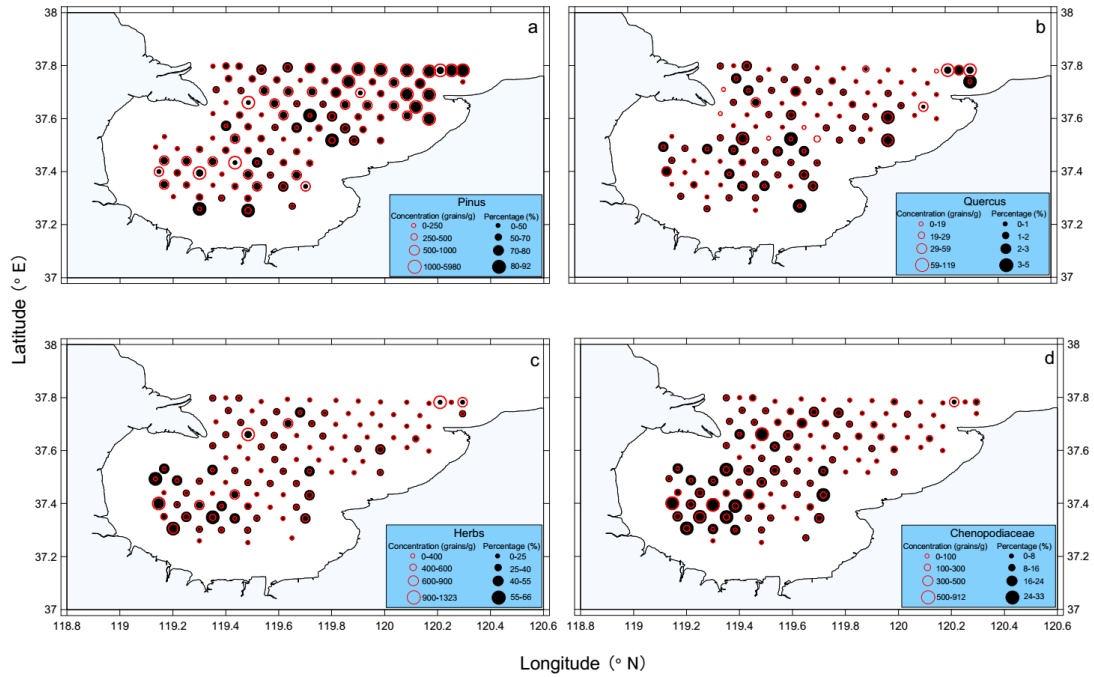


Figure 4: Spatial distribution of modern pollen percentage (black solid circle, %) and concentration (red open circle, grains/g) in Laizhou Bay, Bohai Sea (modified from Yang et al., 2016).

Byun, J.G., Lee, W.K., Kim, M., Kwak, D.A., Kwak, H., Park, T., Byun, W.H., Son, Y., Choi, J.K., Lee, Y.J., Saborowski, J., Chung, D.J., Jung, J.H.: Radial growth response of *Pinus densiflora* and *Quercus* spp. To topographic and climatic factors in South Korea, *J. Plant. Ecol.*, 6, 380–392, 2013.

Chen, W., Wang, W.M.: Middle-Late Holocene vegetation history and environment changes revealed by pollen analysis of a core at Qingdao of Shandong Province, East China, *Quat. Int.*, 254, 68–72, 2012.

Hao, Q., Liu, H.Y., Liu, X.: Pollen-detected altitudinal migration of forests during the Holocene in the mountainous forest–steppe ecotone in northern China, *Palaeogeogr. Palaeoclimatol. Palaeoecol.*, 446, 70–77, 2016.

Jia, Y.H., Li, D.W., Yu, M., Zhao, X.C., Xiang, R., Li, G.x., Zhang, H.L., Zhao, M.X.: High- and low-latitude forcing on the south Yellow Sea surface water temperature variations during the Holocene. *Global. Planet. Change.*, 182, 103025, 2019.

Korea Forest Service: Statistical Yearbook of Forestry. Daejeon, Korea: KFS, 2011.

Kim, C., Park, J.H., Jang, D.H.: Changes of the forest types by climate changes using satellite imagery and forest statistical data: a case in the Chungnam Coastal Ares, Korea, *J. Environ. Impact. Asses.*, 20, 523–538, 2011.

Li, C.Y., Yan, L.Q., Han, T.X.: Research on composition of wetland vegetation in Shandong, *Shandong Forest Sci. Tech.*, 4, 27–29, 2007. (in Chinese with English abstract)

Li, J., Yang, S.X., Shu, J.W., Li, R.H., Chen, X.H., Meng, Y.K., Ye, S.Y., He, L.: Vegetation history and environment changes since MIS 5 recorded by pollen assemblages in sediments from the western Bohai Sea, Northern China. *J. Asian. Earth. Sci.*, 187, 104085, 2020.

- Li, M.Y., Zhang, S.R., Xu, Q.H., Xiao, J.L., Wen, R.L.: Spatial patterns of vegetation and climate in the North China Plain during the Last Glacial Maximum and Holocene climatic optimum. *Sci. China. Earth. Sci.*, 62, 1279-1287, 2019.
- Li, X.Q., Zhou, J., Shen, J., Weng, C.Y., Zhao, H.L., Sun, Q.L.: Vegetation history and climatic variations during the last 14 ka BP inferred from a pollen record at Daihai Lake, north-central China. *Rev. Palaeobot. Palyno.*, 132, 195– 205, 2004.
- Ren, G.Y., Zhang, L.S.: A preliminary mapped summary of Holocene pollen data for northeast China. *Quaternary. Sci. Rev.*, 17, 669-688, 1998.
- Stebich, M., Rehfeld, K., Schlütz, F., Tarasov, P.E., Liu, J.Q., Mingram, J.: Holocene vegetation and climate dynamics of NE China based on the pollen record from Sihailongwan Maar Lake, *Quat. Sci. Rev.*, 124, 275–289, 2015.
- Sun, A.Z., Feng, Z.D.: Climatic changes in the western part of the Chinese Loess Plateau during the Last Deglacial and the Holocene: A synthesis of pollen records, *Quat. Int.*, 372, 130–141, 2015.
- Xu, D.K., Lu, H.Y., Chu, G.Q., Wu, N.Q., Shen, C.M., Wang, C., Mao, L.M.: 500-year climate cycles stacking of recent centennial warming documented in an East Asian pollen record. *Sci. Rep.*, 4, 3611, 2014.
- Xu, Z.J., Zhang, X.L., Zhang, Z.H., Zhang, W.: Analysis of the biodiversity characters of coastal wetlands in southern Laizhou Bay, *Ecol. Env. Sci.*, 19(2), 367–372, 2010. (in Chinese with English abstract)
- Yi, S., Saito, Y., Oshima, H., Zhou, Y.Q., Wei, H.L.: Holocene environmental history inferred from pollen assemblages in the Huanghe (Yellow River) delta, China: climatic change and human impact, *Quat. Sci. Rev.*, 22, 609–628, 2003.
- Zhang, J.Y., Li, J., Yan, Y., Li, J.J., Wan, X.Q.: A 1000-year record of centennial-scale cyclical vegetation change from Maar Lake Sanjiaolongwan in northeastern China. *J. Asian. Earth. Sci.*, 176, 315–324, 2019.

Question 6.

Abstract LINES 14/15: ‘Nevertheless. . . remain sparse.’ This sentence implies that this is generally the case, but there are numerous studies from other regions regarding this aspect. Also ‘long-term’ may be confusing here since the presented record does not even span the whole Holocene. Sentences like this one might perhaps be completely removed.

Answer:

We agree with the advice. We have deleted this sentence in the revised manuscript.

Question 7.

LINE 29 and following: If I did not completely miss anything, the age model is quite unsure between 3000 and 0 years BP (see general comments), and *Pinus* (excluding on

peak that might be a taphonomical signal, s.a.) seems to be decreasing, compare authors' own results (4.2.3).

Answer:

Special thanks for this constructive advice. We agree with this comment. There may be sedimentation hiatus in the depth of 56-34 cm (3000 yr BP-1855 AD). We made a detailed answer in *Question & Answer 2*. In the revised manuscript, we rewrote this part and gave a new discussion.

Question 8.

LINE 30: I understand this that way that the authors call the *Quercus* percentages a 'temperature index', which is very keen!

Answer:

Thanks for this good comment. We changed the sentence 'The pollen-based temperature index indicated that...' into '*Quercus/Pinus* ratio and *Quercus* percentage results indicated that...'.

Question 9.

Introduction LINES 59/60 While the abbreviations YR and BS are already explained in the abstract, maybe they should be explained again in the main text?

Answer:

Thanks for this good comment. We made a correction of the abbreviations YR and BS in the main text.

Question 10.

Climate and vegetation LINE 103 '... annual mean air temperature is 7.5-14.0 °C...' Quite a wide range for an average temperature.

Answer:

Thank you. We made correction to this sentence. '*The annual mean air temperature is 9.5-13.1 °C (Qiao et al., 2012).*'

408 Qiao, F.L., Gan, Z.J., Sun, X.P.: Regional oceanography of China seas-physical oceanography. China
409 Ocean Press, 2012.

410

411 **Question 11.**

412 LINE 109 Perhaps ‘Quercus dentata’ ?

413 **Answer:**

414 We are sorry for the spelling error. We made correction to this mistake.

415

416 **Question 12.**

417 Palynological and grain size sample analysis LINE 133: Lycopodium in italics

418 **Answer:**

419 We are sorry for the spelling error. We made correction to this mistake.

420

421 **Question 13.**

422 LINE 134: Since KOH also degrades pollen, it should be mentioned how long it was
423 used and if all samples were exposed for an identical time interval.

424 **Answer:**

425 We are sorry for the missed information. We added the detailed information in the
426 revised manuscript. ‘*The samples were boiled in 10% KOH solution for 5 min to*
427 *remove humic acids.*’

428

429 **Question 14.**

430 LINE 137: ‘palynomorph sum’ – is the pollen sum meant? If also dinocysts and
431 other palynomorphs have been counted, this should be mentioned here.

432 **Answer:**

433 Thank you. ‘palynomorph sum’ is the pollen and spore sum meant. We have
434 changed ‘palynomorph sum’ to ‘sum of pollen spores’ .

435

436 **Question 15.**

437 LINE 137: ‘exotic pollen method. . .’ The whole sentence seems a little queer to

me, and if Lycopod spores were used, I find the term ‘pollen’ misleading in this context.

Answer:

Thanks for this advice. We have changed this sentence to ‘Pollen concentrations were calculated based on counts of *Lycopodium* spores added to the preparations’.

Question 16.

Chronological model LINE 159: and following: It should be explained which objects were used for the dating (ideally the specific species should be mentioned). Either here or in the discussion it should be discussed what may have caused the discrepancies and why the authors trust the other AMS radiocarbon dates.

Answer:

Thanks for this good advice. We totally agree with the referee. We added some detailed information about the materials for dating in the revision Table 1. ‘The materials for dating are mixed benthic foraminifera.’

Based on the comparison of the sediment rate of our core and nearby cores, we speculate that there may be sedimentation hiatus between 3000 a BP and 1855 AD, and the age at 129 cm depth may not be reliable (See details in *Question & Answer 2*).

Question 17.

Palynological Zone 1 LINE 174: ‘pollen’ is a singular tantum, a plural may only be appropriate if one mentions different pollen types (but even then, ‘pollens’ should better be avoided – occurs again later in the MS).

Answer:

We are sorry for the spelling error. We made correction to this mistake.

Question 18.

Line 178: The MS should be consistent concerning grains/g and grains g⁻¹.

Answer:

We are sorry for the spelling error. We made correction to this mistake.

468

469 **Question 19.**

470 Palynological Zone 2 LINE 186: ‘decline’ (Plural)

471 **Answer:**

472 We are sorry for the spelling error. We made correction to this mistake.

473

474 **Question 20.**

475 LINE 193: Here, NAPs may be appropriate, but I would still suggest to write NAP.

476 **Answer:**

477 We are sorry for the spelling error. We made correction to this mistake.

478

479 **Question 21.**

480 LINE 197: ‘percentage frequency’ sounds/reads strange – percentage implies
481 relative frequency. . . (occurs again later in the MS)

482 **Answer:**

483 We are sorry for the spelling error. We changed ‘percentage frequency’ to
484 ‘percentage’ .

485

486 **Question 22.**

487 Key terrestrial. . . LINE 237: The second sentence sounds/reads strange, and phrases
488 like ‘It is worth noting’ should be avoided – if it was not worth noting, why should
489 one mention it.

490 **Answer:**

491 Thanks. We deleted ‘It is worth noting that’ in the revised MS.

492

493 **Question 23.**

494 LINE 238: There have been many earlier studies which revealed this effect. Perhaps it
495 would be good to add ‘, also for Asian regions’ or something similar after ‘Previous
496 studies’ , or you should cite one older study dealing with the effect.

497 **Answer:**

Thanks for this good advice. We cited two older study (Mudie, 1982; Mudie and Mc Carthy, 1994) to make this expression more clear.

Question 24.

LINE 257: The last sentence seems useless to me.

Answer:

We agree with this point. We have deleted this sentence in the revised manuscript.

Question 25.

Sedimentary records. . . LINE 279: I think these sentences can be significantly condensed. And in this paragraph, the aspect of pollen grain degradation via oxidation would be worth mentioning.

Answer:

Thanks the referee for the suggestion. We rewrote this part in the revised MS.

Question 26.

LINE 281: amount I have not checked the following paragraphs in detail - this should be done by a reviewer with sedimentological expertise. Concerning the interpretation itself, several parts are convincing and I appreciate how the earlier studies are incorporated, but the aspects I discussed in the general remarks should be included. I am particularly surprised about the precise ages given in LINE 426 and LINE 439 - it is not clear to me how 1000 a BP have been determined.

Answer:

Thanks for this good advice. We totally agree with the referee. Please See details in *Question & Answer 2*.

Question 27.

Code/Data availability There are so many options to upload data in an appropriate way these days, but people can change positions, move to other countries or even change their career, therefore, it seems inappropriate to me to name one e-mail address here!

Answer:

Thanks for this good advice. We agree with this advice. We will upload all the data of this study by the suggested gateway (such as the doi address recommended by the journal *Climate of the Past*) when needed.

Question 28.

Author contribution are all aspects mentioned here appropriate to justify being added as co-author?

Answer:

Thanks for the remind. We checked the information again and confirmed all co-authors' contribution.

Question 29.

Table 1: The ages at 119 and 129 have the same calibrated age (probably the one for 119 is wrong?).

Answer:

We are sorry for the spelling error. We made correction to this mistake.

Question 30.

Figures: It seems that genus and species names are not always in italics.

Answer:

We are sorry for the spelling error. We made correction to this mistake.

Question 31.

Figure 8: In addition to my problems with the age model of the core and the use of Quercus as 'temperature index', the labels in this figure are inconsistent. It should be added that the Quercus curve is from core CJ06-435 (if it is shown anyway after revision). It should be added where curve f is from. These are only a few example. . . all labels should say what it is shown and where the record is from (if the data is based on a specific core/region).

Answer:

Thanks for this good advice. We redraw figure 8 and corrected these mistakes.

Reply to Referee #2:

This is an interesting paper that provides a better understanding about the vegetation changes during Holocene in the Bohai Sea region in response to climate change and hydrological processes. Especially it reveals that two rapid and abrupt changes in salt marsh vegetation are linked with the river-system changes.

Thank you for the excellent comments and constructive suggestions for improving our MS. Thanks again for giving this paper a golden chance to be reconsidered for publication in Climate of the Past.

Question 1.

In particular, the Introduction, Geographical settings, Climate and vegetation, materials and methods and discussion are generally well written and easy to follow, but the results need to be more clear and concise and express the key findings of this study including the pollen and spore concentrations.

Answer:

Thanks for this comment. We agree with this and in the revised manuscript we rewrote some of the sections. We hope the new manuscript will be more clear and readable.

Question 2.

Use ages in lieu of depths to express different pollen zones and key features as this paper is mostly focused on timescale not depth and the readers are not supposed to remember depth wise ages.

Answer:

Thanks for this good advice. In the revised manuscript ages information have been added into the pollen zone.

588

589 **Question 3.**

590 Besides, considering grammar, there are several problems with subject-verb
591 agreement, singular and plural expressions, and less use of cohesive devices. However,
592 these problems could be improved with an English language expert.

593 **Answer:**

594 We are sorry for the grammar and language errors. We have invited a professional
595 to modify the language and we have made lots of correction in the revised manuscript.

596

597 **Question 4.**

598 Page 3, line 60: As I know, the Yellow River is the largest sediment transport river in
599 the world, please check this point.

600 **Answer:**

601 We are sorry for this ambiguous expression.

602 According to Milliman and Meade (1983) the average sediment discharge of the
603 Ganges Brahmaputra River, Yellow River and Amazon River are 1.67×10^9 t/a, $1.08 \times$
604 10^9 t/a and 0.9×10^9 t/a, respectively. While result from Meade (1996) reported that the
605 average sediment discharge of these rivers are $(0.9-1.2) \times 10^9$ t/a (Ganges/Brahmaputra
606 river), 1.1×10^9 t/a (Yellow River) and $(1.0-1.3) \times 10^9$ t/a (Amazon River), respectively.
607 In the primary manuscript, we proposed that "The YR, as the second largest river in the
608 world in terms of sediment discharge (Milliman and Meade, 1983) ".

609 In order to avoid this inaccurate introduce, we changed the sentence "*The YR, as*
610 *the second largest river in the world in terms of sediment discharge*" to "*The Yellow*
611 *River (YR), as one of the largest river in the world in terms of sediment discharge*" in
612 the revised manuscript.

613

614 **Question 5.**

615 Page 3, line 72: Before using Acronym for the first time is not correct. Although AMS
616 is a very common acronym, I' ll suggest to use Accelerator Mass Spectrometry (AMS)
617 and then use AMS.

618 **Answer:**

619 We are sorry for the spelling error. We made correction to this mistake.

620

621 **Question 6.**

622 Page 5, line 118: “core collection” could be substituted by “Coring” .

623 **Answer:**

624 Thanks for the Referee’s careful review. We changed "core collection" to "Coring".

625

626 **Question 7.**

627 Page 5, line 123: check the acronym “NIGLAS” . Is it correct?

628 **Answer:**

629 We are sorry for the spelling error. The correct term is "Nanjing Institute of
630 Geography and Limnology, Chinese Academy of Sciences (NIGLAS) ".

631

632 **Question 8.**

633 Page 5, line 125: Did you identify the foraminifera? If so, provide their names for a
634 better understanding, and why only 10 samples were selected? Provide an explanation.

635 **Answer:**

636 Actually we did no work on foraminifera identification. One importance reason is
637 that foraminifera is quite scarce in this kind of shallow water coastal continental shelf.
638 Indeed, neither of the single species of foraminifera is enough for AMS¹⁴C dating in
639 our core. We had to mixed all kinds benthic foraminifera for dating (Detailed introduce
640 was added in the revised Table 1). Even though, some of the layers are not fit for dating
641 because there were almost no foraminifera. Therefore, we selected only 10 samples,
642 and we have tried our best.

643

644 **Question 9.**

645 Page 6, line 132: Did you use wet or dried samples? Mention it.

646 **Answer:**

647 Thanks for this good advice. All samples for pollen and spore analysis were dried

at 60° C and quantified precisely. We added this message in the revised manuscript.

Question 10.

Page 6, line 133: *Lycopodium* needs to italicize. How many *Lycopodium* spores were in the standard tablet?

Answer:

We are sorry for this mistake. The standard *Lycopodium* tablet (Batch 483216) is made by Lund University with a high standard. As mentioned in the **Certification**, each tablet contains $18,583 \pm 764$ *Lycopodium* spore.

Question 11.

Page 6, line 136: How many pollen and spore gains have you counted for each samples?

Answer:

Thank you. A minimum of 200 pollen grains were counted for each sample.

Question 12.

Page 6, line 134: KOH is highly corrosive and can degrade the pollen and spores if exposed for a long time. So, you need to clarify here, how long time you used the KOH.

Answer:

This is a good advice. We agree the point that KOH is highly corrosive and can degrade the pollen. In order to remove humic acids in the sediment, the samples were boiled in 10% KOH solution for 5 min .We added this necessary message in the revised manuscript.

Question 13.

Page 6, line 137: How many pollen and spore were counted for each sample? You need to mention it.

Answer:

Thank you. A minimum of 200 pollen grains were counted for each sample.

Question 14.

Page 6, line 138: In figure, there is CONISS. But, in this section there is no explanation of using CONISS and which software have you used for the graphs and CONISS. Make a clarification here with appropriate references. In addition, please, provide the formula used for palynomorph concentration calculation.

Answer:

Thanks for this constructive comment.

The pollen diagram was plotted using *Tilia program*. The pollen assemblage zones were divided based on the results of a constrained cluster analysis (*CONISS*) within Tilia. The palynomorph concentrations of per gram sediment (*PCP*) were calculated as the follow equation:

$$PCP = \frac{18583}{Lycopodium \text{ number per slide}} * \frac{\text{Pollen or Spore Counts per slide}}{\text{Net weight of dry sample}}$$

Question 15.

Page 6, line 142: the expression is wrong. It should be mol/L or simply M. That is 1.0 mol/L HCl or 1.0 M HCl.

Answer:

We are sorry for the spelling error. We made correction to this mistake.

Question 16.

Page 7, line 152: be consistent using Pb isotopic expressions throughout the manuscript.

Answer:

Thanks for this good advice. We have changed $^{210}\text{Pb}_{\text{ex}}$ to excess ^{210}Pb throughout the revised manuscript.

Question 17.

Page 7, line 170: In figures 3, 4, there are sub-zones also. Make the sentence clear by mentioning how many major and sub-zones there are.

Answer:

Thanks for this good advice. We agree with this point. In the revised manuscript, we added the information "With the aid of CONISS, the whole sequence was vertically divided into three zones, with zone 2 further divided into subzones 2a, 2b, 2c and 2d. "

Question18.

Page 7, line 172: In text it is "Palynological zone", but in Figures it is only "Zone". Be consistent using it. I' ll suggest to use "Palynological zones" in the figure too. You have mentioned only the depth range. Include the ages also, like Palynological zones 1 (271 – 156 cm; 10000-6000 a BP).

Answer:

Thanks the Referee's careful review and good advice. We used "Palynological zones" in the revised figure. Accordingly, we made some revision in the related text.

Question 19.

Page 8, line 176: Which type of abundance? Absolute or relative? make it clear.

Answer:

We are sorry for this ambiguous expression. Here "abundance" refers to the "relative abundance". We made correction in the revised manuscript.

Question 20.

Page 8, line 185: This sentence need to make clear. Instead of "From 156 to 128 cm..." use "From depth of 156 to 128 cm...." elsewhere.

Answer:

Thanks for this kindly advice. We changed "From ** into *** cm... " to "From depth of ** to *** cm... " in this sentence and throughout the revised manuscript.

Question 21.

Page 9, line 224: This word "our" is less formal and overused here in this manuscript. Try to limit its use in the manuscript. There are several other expressions used instead of "our core, our study, our data, and so on".

Answer:

We appreciate the Referee for the language advice. We polished the writing of this manuscript and we hope it is more readable.

Question 22.

Page 11, line 269: “Figure 3 and 6e” should be replaced by “Figures 3 and 6e” as you are referencing two figures. Correct it elsewhere in the manuscript.

Answer:

We are sorry for the spelling error. We made correction to this mistake.

Question 23.

Section 5.5 Holocene temperature variations in North China and possible driving mechanisms: Why have you chosen *Quercus* as a temperate index? Provide and discuss the reasons of using it as a proxy for temperate index.

Answer:

We are grateful for this constructive comment. As this comment was also suggested by the *Referee #1 (Question 5, Answer (2))*.

Quercus has many species in the world. Different response of *Quercus* growth to climate in different region. *Quercus* mainly composed of *Q. acutissima*, *Q. mongolica*, and *Q. liaotungensis* in the land areas surrounding the Bohai Sea. Among these, *Q. acutissima* and *Pinus densiflora* forests develop in the low mountains and hilly area of Shandong Peninsula. *Q. mongolica*, *Q. acutissima* and *P. densiflora* develop in the Liaodong Peninsula (Li et al., 2007; Xu et al., 2010).

It's worth noting that the pollen assemblages in marine surface sediments from the Laizhou Bay revealed that higher concentrations of *Quercus* and *Pinus* pollen distributed in the east of Laizhou Bay, and lower concentrations in the nearshore area outside the estuary of the Yellow River (Figure 1a and b). The distribution of *Quercus* and *Pinus* pollen concentration in surface sediment shows a clearly increasing shoreward the Shandong Peninsula and it is a good indicator for source tracing. In the low mountains and hilly area of Shandong Peninsula, the vegetation is characterized

chiefly by *Q. acutissima* and *P. densiflora* forests. Modern research found that incremental temperature had positive impacts on radial growth of *Q. acutissima* and negative impacts on that of *P. densiflora* (Byun et al., 2013). For example, with the rise of annual mean temperature, *Q. acutissima* forests have naturally increased by approximately 1.13% in South Korea from 1996 to 2010, while *P. densiflora* decreased by 4% (Korea Forest Service, 2011; Kim et al., 2011). Therefore, the variations of *Quercus* and *Pinus* pollen from Shandong Peninsula may be related to temperature change.

Except Shandong Peninsula, pollen from other regions around Laizhou Bay (such as Liaodong Peninsula) may also be transported to the Laizhou Bay, and deposited in core CJ06-435.

Previous studies revealed that *Quercus* and *Pinus* were the dominant components of the forests in northeast China (including the land areas surrounding the Bohai Sea) during the Holocene. The variation of *Quercus* and *Pinus* contents were closely related to the change of temperature (Ren and Zhang, 1998; Li et al., 2004; Xu et al., 2014; Zhang et al., 2019). Ren and Zhang (1998) investigated pollen data from Northeast China and found that *Quercus* and *Ulmus* were the dominant components of the forests in northeast China between 10 and 5 ka, while *Pinus* were much more sparse, indicating a warmer and drier summers in northeast China for the early to mid-Holocene. A high-resolution 1000-year pollen record from the Sanjiaowan Marr Lake (42° 22' 16" N, 126° 25' 39" E) in northeastern China revealed that *Quercus* is a effective indicator for temperature reconstructing. Several notable cold periods, with lower *Quercus* frequencies, occurred at approximately 1200 AD, 1410 AD, 1580 AD, 1770 AD and 1870 AD (Zhang et al., 2019). Another 5350-year pollen record from an annually laminated maar lake (42°18.0' N, 126°21.5' E) revealed a decrease of *Quercus* and an increases of *Pinus* component, indicated a cooling trend during the past 5350 years (Xu et al., 2014).

So, we suggested that *Quercus* is a suitable pollen type for indicating temperature variations in our study region.

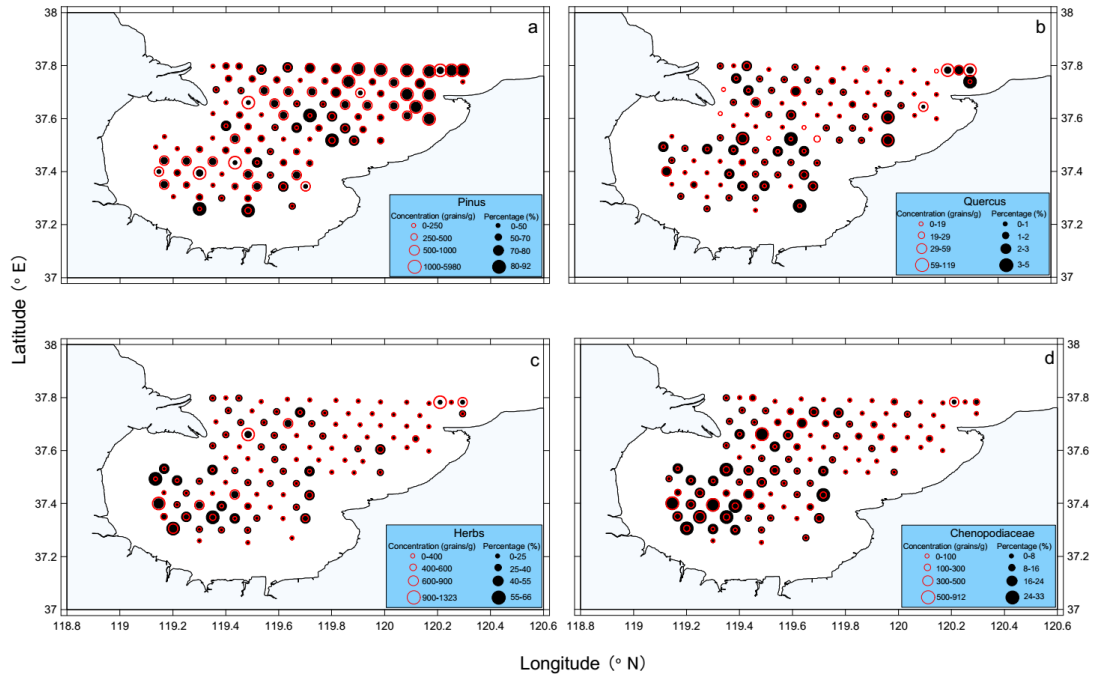


Figure 1: Spatial distribution of modern pollen percentage (black solid circle, %) and concentration (red open circle, grains/g) in Laizhou Bay, Bohai Sea (modified from Yang et al., 2016).

Question 24.

Section 5.4 Palaeovegetation reconstruction and its climate significance: This section need more careful considerations interpreting paleovegetation and paleoclimate. Make comparisons and combination with the findings of other nearby cores in Bohai Sea area. Although there are several cited references, they are not sufficient to establish your findings. What I mean that you need to elaborately discuss your findings and other' s findings.

Answer:

Thanks for this constructive comment. We agree with this point that more detailed discussion and key references should be take consideration for better interpreting paleovegetation and paleoclimate.

We rewrote this part in the revised manuscript. we gave a more detailed discussion of pollen percentage and concentration, the ecology and spread characteristics of main pollen species in core CJ06-435, paleovegetation and paleoclimate evolution of the study region and correlation and teleconnection with other findings in north China (such

as Ren and Zhang, 1998; Yi et al., 2003; Chen et al., 2012; Stebich et al., 2015; Sun and Feng, 2015; Hao et al., 2016; Li et al., 2019; Li et al., 2020; etc.). We hope the revised part will be more logical and readable.

Question 25.

Page 21, line 515, 517: YR in this paper has two meanings: hydrological and Yellow River. Please differentiate them.

Answer:

Thanks for this good advice. We have changed "hydrological (YR) " in line 515 to "hydrological (the shift of YR channel) ".

Question 26.

In Table 1, the ages at depth of 119 and 129 cm are not consistent. Check and revise it. Instead of “mixed foraminifera” mention specific names and if possible the species names of them. In terms of the figures they are generally good, although you need to revise them and make more clear to understand even to a person outside of this research arena.

Answer:

Firstly we are sorry for the mistake ("*the ages at depth of 119 and 129 cm are not consistent*"). We corrected this mistake in the revised manuscript.

For the second question, actually we did no work on foraminifera identification. Moreover, neither of the single species of foraminifera is enough for AMS¹⁴C dating in our core. We had to mixed all kinds benthic foraminifera for dating. So, the materials for dating are mixed benthic foraminifera (Detailed introduce was added in the revised Table 1, we hope this revision is clear.).

Question 27.

Figure 1: Figure 1 (a) can be represented in terms of vegetation map, core locations and Figure 1 (b) can be represented along with sea bed topography to make it more interactive. Please, think about it.

Answer:

Thanks for this good and constructive advice. We added an additional map illustrating the vegetation of the relevant area around the Bohai Sea in the revised MS. We redraw the figure 1(b) and added the information of water depth and topography in the revised figure 1(b).

Question 28.

Figures 3 and 4: The species names are not italicized. Provide a classification of the taxa showed in the figure into trees, ferns, and herbs (upside of the graph). In addition, give a classification of arboreal, non-arboreal pollen types in the figures (may be at the bottom part). It will make the figure easier to interpret.

Answer:

Special thank for this kindly comment. We redraw the figures and all species names have been changed to italicized. Also, we gave classifications of arboreal, non-arboreal pollen types in the figures.

Question 29.

Figure 5: There is no information about the position of land and Rivers. Point out the names in the maps for a clear understanding.

Answer:

Yes, we agree with the Referee. We added the information about the position of land and rivers in figure 5.

Question 30.

Figure 8: The unit of Age is not consistent here. Sometimes you have used cal kyr BP, ka BP, or cal. (a BP). Be consistent and use the instructions of the journal to express ages.

Answer:

Special thanks for this kindly and careful review. Indeed, there were many inconsistent use of age expression throughout the primary manuscript. We are very

sorry for this kind of mistakes and ignorance. In the revised manuscript, we have
checked the expressions thoroughly. We hope we have eliminated all this kind of errors.

A list of all relevant changes made in the manuscript

1. Authors list	Added an author
2. lines 14-17	Response to question 6 of the referee 1
3. line 32	Response to question 7 of the referee 1
4. line 33	Response to question 8 of the referee 1
5. lines 66-67	Response to question 9 of the referee 1
6. lines 67-68	Response to question 4 of the referee 2
7. lines 81-82	Response to question 5 of the referee 2
8. lines 118-119	Response to question 10 of the referee 1
9. line 126	Response to question 11 of the referee 1
10. line 137	Response to question 6 of the referee 2
11. lines 142-143	Response to question 7 of the referee 2
12. lines 153-154	Response to question 9 of the referee 2
13. line 156	Response to question 10 of the referee 2
14. line 156	Response to question 12 of the referee 1
15. lines 160-161	Response to question 11 of the referee 2
16. line 158	Response to question 12 of the referee 2 and question 13 of the referee 1
17. lines 161-166	Response to question 14 of the referee 2
18. line 164	Response to question 14 of the referee 1
19. line 161-163	Response to question 15 of the referee 1
20. line 170	Response to question 15 of the referee 2
21. line 182	Response to question 16 of the referee 2
22. lines 192-201	Response to question 16 of the referee 1
23. line 227	Response to question 17 of the referee 1
24. line 232	Response to question 18 of the referee 1
25. line 238	Response to question 19 of the referee 1
26. line 246	Response to question 20 of the referee 1
27. line 250	Response to question 21 of the referee 1
28. lines 220-222	Response to question 17 of the referee 2
29. lines 230-231	Response to question 19 of the referee 2
30. line 236	Response to question 20 of the referee 2
31. lines 203-266	We rewrote the section of "results" for response to question 1 of the referee 2
32. lines 270-303	Response to question 5 of the referee 1
33. line 319	Response to question 24 of the referee 1
34. lines 326-327	Response to question 23 of the referee 1
35. lines 335-358	Response to question 1 of the referee 1
36. lines 514-528	Response to question 2 of the referee 1
37. line 540	Response to question 3 of the referee 1
38. lines 579-596	Response to question 26 of the referee 1
39. lines 705-710	Response to question 28 of the referee 1
40. lines 512-604	We rewrote the section of "5.4. Palaeovegetation reconstruction and its

	climate significance” for response to question 24 of the referee 2
41. lines 606-677	We rewrote the section of “5.5. Holocene temperature variations in north China and possible driving mechanisms” for response to question 5 of the referee 1
42. figures 1 and 2	Response to question 27 of the referee 2
43. figures 4 and 5	Response to question 28 of the referee 2
44. figure 6	Response to question 29 of the referee 2
45. figure 9	Response to question 30 of the referee 2 and question 31 of the referee 1

906

907

908

909

910

911

912

913

914

915

916

917

918

919

920

921

922

923

924

925

926

927

928

929

Holocene vegetation dynamics in response to climate change and hydrological processes in the Bohai region

Chen Jinxia^{a,b,*}, Shi Xuefa^{a,b,*}, Liu Yanguang^{a,b}, Qiao Shuqing^{a,b}, Yang Shixiong^{c,d}, Yan Shijuan^{a,b},
Lv Huahua^{a,b}, Li Jianyong^e, Li Xiaoyan^{a,b}, Li Chaoxin^{a,b}

^a Key Laboratory of Marine Geology and Metallogeny, MNR, Qingdao 266061, China

^b Laboratory for Marine Geology, Qingdao National Laboratory for Marine Science and Technology, Qingdao 266061, China

^c Key Laboratory of Coastal Wetland Biogeosciences, China Geological Survey, Qingdao 266071, Shandong, China

^d Laboratory for Marine Geology, Qingdao National Laboratory for Marine Science and Technology, Qingdao, 266061, China

^e College of Urban and Environmental Sciences, Northwest University, Xian, 710127, China

* Corresponding author at: Key Laboratory of Marine Geology and Metallogeny, MNR, Qingdao 266061, China.

E-mail address: jinxiachen@fio.org.cn (J. Chen); xfshi@fio.org.cn (X. Shi).

ABSTRACT

Coastal vegetation both mitigates the damage inflicted by marine disasters on coastal areas and plays an important role in the global carbon cycle (i.e. blue carbon). Nevertheless, detailed records of changes in coastal vegetation composition and diversity in the Holocene, coupled with climate change and river evolution, remain unclear. To explore vegetation dynamics and their influencing factors on the coastal area of the Bohai Sea (BS) during the Holocene, we present high-resolution pollen and sediment grain size data obtained from a sediment core of the BS. The results reveal that two rapid and abrupt changes in salt marsh vegetation are linked with the river-system changes. Within each event, a recurring pattern—starting with a decline in Cyperaceae, followed by an increase in *Artemisia* and Chenopodiaceae—suggests a successional process that is determined by the close relationship between Yellow River (YR) channel shifts and the wetland community dynamics. The phreatophyte Cyperaceae at the base of each sequence indicate lower saline conditions. Unchannelized river flow characterized the onset of the YR channel shift, caused a huge river-derived sediment accumulation in the floodplain, and destroyed the sedges in the coastal depression. Along with the formation of a new channel, lateral migration of the lower channel stopped, and a new intertidal mudflat was formed. Pioneer species (Chenopodiaceae, *Artemisia*) were the first to colonize the bare zones of the lower and middle marsh areas. In addition, the pollen results revealed that the vegetation of the BS land area was dominated by broadleaved forests during

the early Holocene (8500–6500 a BP) and by conifer and broadleaved forests in the middle Holocene (6500–3500 a BP), which was followed by an expansion of broadleaved trees (after 3500 a BP). The pollen record indicated that a warmer early and late Holocene and colder middle Holocene were consistent with previously reported temperature records for East Asia. The main driving factors of temperature variation in this region are insolation, the El Niño–Southern Oscillation and greenhouse gases forcing.

Keywords: Coastal salt marsh; Pollen; Delta superlobe; Temperature; El Niño–Southern Oscillation

1. Introduction

Coastal areas, where cities, populations and industries are clustered, are playing an increasingly critical role in trade globalization (Hemavathi et al., 2019). Because they are located between marine ecosystems and terrestrial ecosystems, coastal areas are prone to many natural hazards such as flooding, storms, and tsunamis (Hou and Hou, 2020). Coastal vegetation, which acts as a natural barrier, is widely distributed in coastal areas and could effectively mitigate the damage caused by marine disasters to the economy and environment of coastal areas (Zhang et al., 2018). Moreover, despite their relatively small global extent (between 0.5 and 1×10^6 km²), coastal vegetation ecosystems, tidal marshes, mangroves, and seagrasses play an important role in the global carbon cycle (Serrano et al., 2019; Spivak et al., 2019). Per unit area, their organic carbon sequestration rates exceed those of terrestrial forests by 1–2 orders of magnitude and contribute ~50% of carbon sequestered in marine sediments (Serrano et al., 2019). Hence, it is important to understand the long-term spatial–temporal dynamics of coastal vegetation, which are favorable for the global carbon cycle research and coastal restoration.

Climatic fluctuation, post glacial sea-level rise and changes in river discharge provoked dramatic habitat changes along coastal areas during the Late Pleistocene and Holocene (Neumann et al., 2010; Cohen et al., 2012; Pessenda et al., 2012; França et al., 2015). Presently, the relationship of sea-level change and coastal vegetation (especially mangrove) evolution has been widely studied by many researchers (e.g. Engelhart et al., 2007; Gonza lez and Dupont, 2009; França et al., 2012; Woodroffe et al., 2015; Hendy et al., 2016). Contrarily, studies on the long-term dynamics of coastal vegetation, coupled with climate change and river evolution, are sparse. During the Holocene, the

global rivers delivered large amounts of material to the ocean, the total suspended sediment delivered by all rivers to the ocean was approximately 13.5×10^9 tons annually (Milliman and Meade, 1983). The material transported by the rivers had huge impacts on the coastal ecosystem. Hence, a deeper understanding of correlations between coastal vegetation and river variables is required to better assess coastal vegetation responses to global warming in the future.

In the coastal areas of the Bohai Sea (BS), vegetation is dominated by warm temperate deciduous broadleaved forests and shrub grasslands (Wang et al., 1993). The Yellow River (YR), as one of the largest river in the world in terms of sediment discharge (Milliman and Meade, 1983), transports large amounts of sediment into the BS every year; hence, it has developed a delta complex in the west coastal region of the BS since 7000 a BP (He et al., 2019). Deposition of the Yellow River delta (YRD) complex resulted in the formation of a vast area of floodplain and estuarine wetland (Xue et al., 1995; Cui et al., 2009; Liu et al., 2009b). Based on the study of coastal vegetation of the BS, it is helpful to understand the spatial and temporal drivers of ecological variability, and thus of the vegetation-climate and river relationship, especially wetland dynamics. However, there have been few studies investigating the vegetation dynamics and their response to climate and river variables in the Bohai region.

Pollen records have been useful in terms of reconstructing vegetation dynamics and environmental changes associated with climatic changes in the geological record (Bao et al., 2007; Cohen et al., 2008; Giraldo-Giraldo et al., 2018). In this study, we carried out a detailed investigation of core sediments from Laizhou Bay, BS. We analyzed pollen and grain size proxies under high resolution and refined the chronology of the core by ^{137}Cs and accelerator mass spectrometry (AMS) ^{14}C dates. With this in mind, the specific objectives of the current research are formulated as follows: (1) to reconstruct the vegetation evolution history in the Bohai region and (2) to tentatively discuss the effects of climate and environment on coastal vegetation (especially wetlands) during the Holocene.

2. Study area

2.1. Geographical settings

The BS, a shallow inland sea in China, is connected with the Yellow Sea through the narrow Bohai Strait (Figure 1). The main rivers flowing into the BS are the YR, Haihe River, Luanhe River,

and Liaohe River. Among these, the YR is the largest and is the main source of sediments in this region. Over the past 2000 years, the YR has annually provided approximately 1.1×10^9 tons of sediment discharged into the BS (Milliman et al., 1987). This immense amount of sediment has resulted in the rapid seaward progradation of YRD, and a rapid change in the location of the main distributaries in the lower delta plain.

The tidal current plays a critical role in the transportation and distribution of sediments in the BS. The tidal currents of the modern BS are dominated by semi-diurnal tides. The velocity of tidal currents varies from 20 to 80 cm/s. Three strong tidal current areas are observed in the northern Bohai Strait, the central part of Bohai Bay, and the eastern part of Liaodong Bay (Huang et al., 1999). In Laizhou Bay close to the core location, the speed of tidal currents is weak (Gu and Xiu, 1996).

The wind waves off the YRD are dominated by the East Asian monsoon and show significant seasonal variations. The prevailing northerly winds are much stronger in winter than the dominant southerly winds in summer. Strong winter winds cause strong wind waves, and thus strong bottom shear stresses which readily erode seabed sediment into water (Yang et al., 2011; Wang et al., 2014; Zhou et al., 2017).

The circulation of the BS is weak, and the mean flow velocity is small. In winter, the predominant extension of the Yellow Sea Warm Current (YSWC) intrudes and crosses the Bohai Strait, moving westward along the central part of the BS and splits into two branches. One branch moves toward the northeast to form a clockwise gyre (Liaoxi Coastal Current [LXCC]), and the other veers southward and then turns eastward along the southern coast to form a counterclockwise gyre (Libei Coastal Current [LBCC]). In summer, the YSWC disappears in the BS, and eddies generated in the BS are stronger than in winter. During this time, the central eddy is missing, the eddy in Laizhou Bay is more pronounced, and the coastal current along the southern and western coastlines of the BS is established (Figure 2; Liu et al., 2015; Yang et al., 2016).

2.2. Climate and vegetation

The Bohai region lies in a zone of warm temperate monsoonal climate with distinctive seasons. The annual mean air temperature is 9.5–13.1 °C. The annual average precipitation is about 600 mm, and 60–70% of the total annual precipitation occurs between June and August (Qiao et al., 2012).

As the Liaodong Peninsula and Shandong Peninsula protrude into the sea, they are clearly

influenced by its proximity and experience sufficient rainfall. There is less rainfall in the mountain area of the northern part (Wang et al., 1993).

The regional vegetation is dominated by warm temperature deciduous broadleaved forests and shrub grasslands. Currently, natural vegetation only remains in the mountain areas because of widespread anthropogenic activities (e.g. cultivation and farming). The predominant deciduous broadleaved species belong to *Quercus*, such as *Q. liaotungensis*, *Q. dentata*, *Q. acutissima*, and *Q. mongolica*. Co-dominant plants are *Pinus*, including *P. densiflora* that grows in the coastal humid area, and *P. tabuliformis* that is distributed in the relatively dry North China plain. In the plain area, apart from *P. tabuliformis*, there are some deciduous broadleaved trees, such as *Ailanthus altissima*, *Koelreuteria paniculata*, and *Morus alba*. Other broadleaved trees, *Betula ermanii*, *Populus tremula*, *Acer* spp., *Tilia amurensis*, and *Carpinus turczaninowii* are distributed in the hills and lowlands (Wang et al., 1993). The coastal wetlands are occupied by herbs and shrubs, such as *Tamarix chinensis*, *Salix matsudana*, *S. integra*, *Phragmites australis*, *Aeluropus*, *Limonium sinense*, *Suaeda glauca*, *Typha orientalis*, and *Acorus calamus* (Wang et al., 1993; Li et al., 2007; Xu et al., 2010).

3. Materials and methods

3.1. Coring, sub-sampling, and chronology

Core CJ06-435 was collected in Laizhou Bay, BS in August 2007 by the R/V *Kan407* of the Shanghai Bureau. The core site is located at 37.50°N, 119.52°E, at a water depth of 14.6 m (Figure 1); the core had a length of 271 cm. In the laboratory, the core was spilt into two sections, photographed, macroscopically described, and sub-sampled.

Isotopes ^{137}Cs and ^{210}Pb were measured employing EG&G Ortec Gamma Spectrometry at the Nanjing Institute of Geography and Limnology, Chinese Academy of Sciences (NIGLAS). The sediment samples were air-dried and pulverized. ^{137}Cs and ^{210}Pb concentrations were then determined from gamma emissions at 662 and 46.5 keV, respectively. In addition, a total of 10 samples consisting of foraminifera were obtained from the core for radiocarbon dating. The radiocarbon dating was conducted at the Woods Hole Oceanographic Institution (WHOI) and Beta Analytic Inc., USA. Radiocarbon dates were corrected for the regional marine reservoir effect ($\Delta R = -139 \pm 59$ years, a regional average value determined for the BS) and calibrated using the Calib 7.04 program (Stuiver et al., 2019) with one standard deviation uncertainty ($1.0 \times \sigma$) (Table 1).

3.2. Palynological and sediment grain size sample analysis

A total of 127 samples were selected for pollen analyses. Each sample was oven-dried at 60 °C for 24 h. The dry-weight of the samples ranged from 2.5 g to 13.9 g. Samples were chemically treated according to the procedure outlined by Faegri and Iversen (1992). Before treatment, a standard tablet of *Lycopodium* spores (mean=18,583±764 spores per tablet) was added to each sample to aid in the calculation of palynological concentrations. Samples were treated with 15% HCl solution to remove carbonates, boiled in 10% KOH solution for 5 min to remove humic acids, then treated with 40% HF to remove silicates. The residue was mounted in glycerin jelly. Fossil pollen was identified and counted with a light microscope at 400× magnification. A minimum of 200 pollen grains were counted for each sample. The palynological concentrations of per gram sediment (PCP) were calculated using the follow equation:

$$PCP = \frac{18583}{Lycopodium \text{ number per slide}} * \frac{\text{Pollen or Spore Counts per slide}}{\text{Net weight of dry sample}}$$

The percentage of each pollen type was calculated from the total sum of pollen and spores. The pollen diagram was produced using the Tilia program, and the pollen assemblage zones were divided based on the results of a constrained cluster analysis (CONISS) within Tilia (Grimm, 1987).

Analysis of sediment grain size was performed at 2.0 cm intervals throughout the core using a Malvern Mastersizer 2000 instrument at the laboratory of the First Institute of Oceanography. The chemical procedure of grain size experimental pretreatment was consistent with the procedures described by Chen et al. (2019a). A solution of 30% H₂O₂ and 1.0 mol/L HCl were added to decompose the organic matter and remove carbonates.

4. Results

4.1. Chronological model

Measurements of ¹³⁷Cs and ²¹⁰Pb revealed activity at the top of the profile, indicating the recovery of recently deposited sediments. ¹³⁷Cs is a bomb-derived radionuclide, first appearing in environmental samples at measurable levels around 1954 with the onset of nuclear weapon testing (Kirchner and Ehlers, 1998), and was most prevalent in 1963 (the year of maximum fallout from atmospheric weapon testing) (Palinkas and Nitttrouer, 2007). Sub-surface peaks are not discernible

in ^{137}Cs profiles of core CJ06-435 (Figure 3). However, the deepest onset of ^{137}Cs is an effective marker of the year 1954 (25 cm).

Often, the combined data of ^{137}Cs and excess ^{210}Pb have been used to calculate the sedimentation rates (Wu et al., 2015). Excess ^{210}Pb shows a downward decline owing to the decay of ^{210}Pb when the sediment stably accumulates for an appropriate period, and the excess ^{210}Pb activity could be used to calculate the sedimentation rate. However, the excess ^{210}Pb profiles of core CJ06-435 did not show a clear downward decline trend (Figure 3), and excess ^{210}Pb in the upper parts of the core is not that large when compared with the lower background values. Thus, the ^{210}Pb data seemed to be unsuitable for estimating the sedimentation rate of core CJ06-435. The ^{137}Cs -derived average sedimentation rate was 0.47 cm/yr in the upper 25 cm of core CJ06-435.

The results of AMS radiocarbon dating are shown in Table 1 and Figure 3. Three samples above the 20 cm depth were not included in the age model because their ^{14}C age was anomalously greater than the ^{137}Cs dating. The dating point of 129 cm was eliminated because it appears not to be reliable. According to the result of He et al. (2019), the calculated sedimentation rate (CSR) in the tidal flat and neritic area of the south BS ranged from 0.02 to 0.13 cm/year before 2000 a BP (calculation from cores H9601, H9602, ZK228, and ZK1, Figure 1). If the 129 cm dating is correct, the CSR would be as high as 0.45 cm/yr in the section of 87–129 cm (4801–4894 a BP) for core CJ06-435. It is apparently not reasonable because core CJ06-435 is offshore compared to the other cores (e.g. H9601, H9602, ZK228, and ZK1, Figure 1) reported in previous researches (Xue et al., 1988; Saito et al., 2000; Li et al., 2013). It should have a lower CSR compared to those cores rather than an approximate ten-fold increase in CSR. The calibrated dates of several other samples are plotted against sediment depth and shown in Figure 4.

4.2. Sediment grain size distributions

The grain size parameters and components percentages show distinct variations. The mean grain size and the median grain size both show high values at depths of 271–160 cm, 135–83 cm and 19–0 cm, lower values at a depth of 83–34 cm, and the lowest values at depths of 160–135 cm and 34–19 cm. There was a smaller proportion of clay in the lower profile (271–160 cm) than in the upper profile (160–0 cm, except for the two sections of 160–135 cm and 34–19 cm). The sequences of silt and sand contents showed a strong inverse association. There were high proportions of silt

and low proportions of sand at depths of 271–222 cm, 180–160 cm, 135–83 cm, 40–34 cm and 19–0 cm, lower proportions of silt and higher proportions of sand at depths of 222–180 cm and 83–40 cm, and the lowest proportions of silt and the highest proportions of sand occurred at depths of 160–135 cm and 34–19 cm (Figure 3).

4.3. Palynology assemblage

A total of 71 pollen taxa were identified, among which *Pinus*, *Quercus*, Cyperaceae and *Typha* were the most dominant taxa in the lower part (271–156 cm) of the core, and *Pinus*, *Quercus*, Poaceae, Compositae, *Artemisia*, Chenopodiaceae and Cyperaceae were the most dominant taxa in the upper part (156–0 cm) of the core. With respect to the fern spores, *Selaginella sinensis* and Polypodiaceae were dominant; however, their content was low throughout the core. With the aid of CONISS, the whole sequence was vertically divided into three zones, with zone 2 further divided into subzones 2a, 2b, 2c and 2d (Figures 4 and 5).

4.3.1. Palynological zone 1 (271–156 cm)

The palynological zone 1 was characterized by abundant broadleaved trees pollen, dominated by *Quercus* (mean 18.7%), *Betula*, *Alnus*, *Pterocarya*, Ulmaceae and Moraceae (Figure 4). Percentages of conifer pollen were relatively low compared with other zones: *Pinus* ranges from 19.7% to 45.6% (mean 33.6%), and Taxodiaceae was present only occasionally. Compared to the other zones, the proportions of non-arboreal pollen types, Compositae (mean 1.2%), *Artemisia* (mean 4.2%), and Chenopodiaceae (mean 5.6%) were lowest in this zone, whereas the proportions of Cyperaceae (mean 10.3%) and *Typha* (mean 11.2%) were highest in this zone. The palynological concentrations were high, varying between 6050 and 237 grains/g (Figure 5).

4.3.2. Palynological zone 2 (156–30 cm)

Palynological zone 2 was divided into four subzones:

From depth of 156 to 128 cm (subzone 2a), the percentage of *Pinus* pollen reached its maximum (mean 46.6%), whereas the percentage of broadleaved trees *Quercus* (16.1–9.5%, mean 14%), *Betula*, *Alnus*, *Pterocarya*, Ulmaceae, and Moraceae decreased to different degrees. The proportions of non-arboreal pollen types, Compositae (mean 2.5%), *Artemisia* (mean 6.6%), and

Chenopodiaceae (mean 7.4%) were higher, whereas the percentages of Cyperaceae (mean 7.2%) and *Typha* (mean 3.1%) declined sharply (Figure 4). Total pollen concentration were lower than in zone 1, especially in the interval of 156–135 cm, where the value of total pollen concentrations (62–1306 grains/g, mean 485 grains/g) was at its minimum in the core (Figure 5).

From depth of 128 to 63 cm (subzone 2b), *Pinus* (49.4–27.3%) and *Quercus* (18.1–7.9%, mean 13.5%) pollen level decreased to a low point, and the relative abundance of *Betula* slightly increased. Occasionally, there were small amounts of *Pterocarya*, Ulmaceae, and Moraceae. Non-arboreal pollen types, Compositae, *Artemisia*, and Chenopodiaceae continuously increased to averages of 3.5%, 6.7%, and 12%, respectively (Figure 4). Pollen concentration increased up to a high abundance (mean 1260 grains/g) in this subzone (Figure 5).

From depth of 63 to 41 cm (subzone 2c), the percentage of *Pinus* pollen started to decrease steadily, and the percentage of *Quercus* (17.4–11.8%, mean 14.8%), *Betula*, *Alnus*, *Pterocarya*, and Ulmaceae pollen slightly increased. Similar to subzone 2b, this subzone had relatively high quantities of non-arboreal pollen such as Compositae, *Artemisia*, and Chenopodiaceae (Figure 4). Pollen concentrations varied between 456 and 1381 grains/g (Figure 5).

In contrast, subzone 2d (41–30 cm) was marked by a sudden decrease in the pollen of *Quercus* (9.8%), and a steep increase in the pollen of *Pinus* (41.1%), even though the percentage of the non-arboreal were the same as those of subzone 2c (Figure 4).

4.3.3. Palynological zone 3 (30–0 cm)

This zone was characterized by the transition from dominance by the pollen of arboreal taxa to non-arboreal types. The percentage of *Pinus* and *Quercus* pollen decreased to the lowest level, averaging approximately 19.7% and 5.5%, respectively. Poaceae, Compositae, *Artemisia*, and Chenopodiaceae pollen increased, with average values of *Artemisia* and Chenopodiaceae reaching up to 24.6% and 21.1%, respectively (Figure 4). The total pollen concentration declined to 188 grains/g in the lower part of the zone (30–19 cm) and then increased slightly (to approximately 621 grains/g) at the top (Figure 5).

5. Discussion

5.1. Key terrestrial palynomorphs proxies of environmental and climatic change

In sediment core CJ06–435, both *Pinus* and *Quercus* pollen were the predominant pollen types among the arboreal taxa. In order to understand the pollen provenance, the pollen records in the surface sediments of Laizhou Bay were studied (Yang et al., 2016), and the concentration and percentage data of main pollen species were presented on a regional map (Figure 6). Pollen results of surface sediments revealed that higher values of *Pinus* and *Quercus* are usually found in the eastern part of Laizhou Bay, and the lowest values of *Pinus* and *Quercus* occur in the nearshore area outside the mouth of the YR (Figure 6a and 6b). The distributions of *Pinus* and *Quercus* pollen in the surface sediments of Laizhou Bay are closely related to the distribution of the nearshore epicontinental vegetation. Except for the YRD, where there is swamp and cultivated land, the epicontinental region of the Laizhou Bay is surrounded by pine and oak forests. Among these, the land to the east of the Laizhou Bay (the Shandong Peninsula) belongs to the southern warm temperate zone and mainly supports a pine–oak forest dominated by *Pinus densiflora* and *Q. acutissima* (Wang et al., 1993). The land to the northeast of the Laizhou Bay (the Liaodong Peninsula) belongs to the southern temperate zone, and it mainly developing a conifer and broadleaved mixed forest dominated by *P. densiflora*, *Q. mongolica* and *Q. acutissima* (Li et al., 2007; Xu et al., 2010). The ubiquitous distribution of these plants on the adjacent terrain explains why *Pinus* and *Quercus* are the most common pollen taxa in Laizhou Bay, and why the highest concentration and percentage of *Pinus* and *Quercus* occurred in the eastern part of Laizhou Bay and the lowest values of *Pinus* and *Quercus* occurred on the nearshore area outside the mouth of the YR.

Previous studies have revealed that *Pinus* and *Quercus* were the most common components of the forests in northeast China (including the land areas surrounding the BS) during the Holocene. The variation of *Pinus* and *Quercus* contents were closely related to the change of temperature (Ren and Zhang, 1998; Yi et al., 2003; Li et al., 2004; Xu et al., 2014; Zhang et al., 2019). Ren and Zhang (1998) investigated pollen data from northeast China and found that *Quercus* and *Ulmus* were the dominant components of the forests between 10000 and 5000 a BP, while *Pinus* were much sparser, indicating warmer and drier summers in northeast China for the early to mid-Holocene. A high-resolution 1000-year pollen record from the Sanjiaowan Marr Lake in northeast China revealed that *Quercus* is an effective indicator for temperature reconstructions. Several notable cold periods, with lower *Quercus* frequencies, occurred at approximately 1200 AD, 1410 AD, 1580 AD, 1770 AD and

1870 AD (Zhang et al., 2019). Another 5350-year pollen record from an annually laminated maar lake in northeast China revealed a decrease of *Quercus* and increases of the *Pinus* component; this indicates a cooling trend during the past 5350 years (Xu et al., 2014). Based on these results, we conclude that the variation of *Pinus* and *Quercus* pollen of core CJ06-435 may be also related to temperature change.

Herb pollen, especially Chenopodiaceae, also occupies an important position in core CJ06-435 (Figure 4). The spatial distribution of herb pollen in surface sediment of Laizhou Bay suggests that a higher percentage and concentration occur in the nearshore area close to the YR estuary and the southwestern part of Laizhou Bay, and a low percentage and concentration are found in the eastern part of Laizhou Bay (Figure 6c and 6d). The YR is the main sediment source of the BS. The annual mean sediment load of the YR was 1.08×10^9 tons before dam construction (Milliman and Meade, 1983), 70–90% of which was deposited and formed a huge delta complex (Zhou et al., 2016). Natural vegetation in the modern YRD are dominated by wetland herbs, including Chenopodiaceae and *Artemisia* (Jiang et al., 2013). Furthermore, under the combined action of the ocean and rivers, alluvial plains and coast plains developed widely along the southern coast of Laizhou Bay. The terrestrial vegetation types in these areas change from a bare intertidal zone to seepweed swamp to reed swamp to cultivated land from the shoreline landward (Xu et al., 2010). Since the transportation distance for herb pollen is normally very short, the pollen percentage and concentration in samples close to the mouth of the YR and the southwestern part of Laizhou Bay are much higher than in other samples (Figure 6c and 6d), indicating that herb pollen of Laizhou Bay is mainly derived from the plant communities of the coastal wetlands.

It is worth noting that the composition of fossil pollen in sediment depends not only on the composition of the vegetation from which the pollen originates but also on pollen dispersion, deposition and preservation. *Pinus* pollen is a bisaccate grain, and has relatively high aerodynamic and hydrodynamic characteristics meaning it can be transported efficiently by wind and water (Sander, 2001; Montade et al., 2011). Previous studies revealed that smaller amount of *Pinus* pollen are found nearshore, and larger amounts are found in the deep ocean (Mudie, 1982; Mudie and McCarthy, 1994; Zheng et al., 2011; Dai et al., 2014; Luo et al., 2014; Dai and Weng, 2015). In Laizhou Bay, the concentration and percentage of *Pinus* pollen followed similar patterns of distribution to broadleaved tree pollen (*Quercus*, *Betula* and *Carpinus*; Yang et al. 2016). However,

in the eastern part of Laizhou Bay, *Pinus* pollen increased in a northeasterly direction away from the coast (Figure 6a). Hence, concerning *Pinus* pollen data, caution is required because climate variation alone may not be responsible for the change of *Pinus* pollen in marine sediment. Aerodynamic and hydrodynamic conditions may also influence the amount of *Pinus* pollen in sediments.

In addition, because different pollen types are not equally well preserved (Havinga, 1967; Cheddadi and Rossignol-Strick, 1995), bias originating from poor preservation should be eliminated before using the net content of pollen grains to reconstruct paleovegetation. In this study, the pollen concentration ranged from 62 to 6050 grains/g. Relatively low pollen concentrations were found in the two sections (160–135 cm and 34–19 cm); this was largely correlated to high sand contents as revealed by the lithology. Especially for the lower section (150–135 cm), the high portion of sand content is consistent with a low pollen concentration and a high percentage of *Pinus* pollen. As the *Pinus* pollen is more resistant to degradation, the variations of total pollen concentration as well as a higher percentage of *Pinus* pollen in this section seem to be related to pollen preservation. But, as shown in Figure 4, the highest percentage of *Pinus* pollen was recorded at a depth of 150–128 cm, with a low value at 148 cm, which is not completely in accordance with the high sand content section in the same core (160–135 cm). Similarly, for the upper section, a high sand content was recorded at a depth of 34–19 cm. However, the percentage of *Pinus* pollen is low in this section, except for a relatively high value at a depth of 23 cm. We thus suggest degradation is not a key point influencing the concentration of pollen and spore in the study area.

Previous research suggests that the sedimentation mechanisms of pollen and spore in marine water is similar to that of sediment with clay and fine silt grain size (Heusser, 1988). A recent investigation on the surface sediment from the BS shows high pollen concentration in sediments with a high proportion of fine particles such as clay and silty clay, while low pollen concentration in sediments with a high proportion of coarser sand particles (Yang et al., 2019). Yang et al. (2019) attributed the low pollen concentration in areas with a high sand content of the BS to the strong hydrodynamic suspension and screening for sediments and pollen. We conclude that the low pollen concentrations in the two sections (160–135 cm, and 34–19 cm), correlated with high sand content, could be attributed to the hydrodynamic conditions rather than degradation.

5.2. Sedimentary records indicative of river channel shifts

The most important geological events in the northern China coast after 7000 a BP were the shift of YR channel and the formation of the YRD. The YR has been easily plugged and breached, and therefore its lower reaches migrated because of its huge sediment load. The shifting of the lower reaches of the YR led to the formation of a new delta superlobe (He et al., 2019). Based on a study of cheniers and historical documents, nine YRD superlobes have been proposed by Xue and Cheng (1989) and Xue (1993) on the western shore of the BS. Among these, superlobe 1 (7000–5000 a BP, He et al., 2019), superlobe 7 (11 AD–1048 AD, Xue, 1993), and superlobe 10 (1855 AD–present) are positioned near the core area in this study. The information about some of these superlobes formation are recorded in core CJ06-435.

As shown in Figures 4 and 7e, herb percentage abruptly increased at 34 cm and 160 cm. Herb pollen in the sediment of Laizhou Bay is mainly derived from the coastal wetlands of the western BS. In 6000–7000 a BP and 1855 AD, the YR emptied into the BS after a natural course shift, forming two huge delta superlobes in the western part of the BS (Saito et al., 2000). Wetland plants are the most important vegetation type in the YRD (Jiang et al., 2013). The development of YRD wetland would change the amounts of herb pollen that was transported to the study site. In addition, the formation of YRD caused the coastline to move closer to the position of the CJ06-435 core. Since most herb plants are small in size, their pollen grains are unable to disperse broadly (Chen et al., 2019b). The migration of the coastline would change the availability of herb pollen to the study site, and hence lead to variations in the amount of pollen. Therefore, combined with the age data, we conclude that the abrupt change of herb pollen percentage at 160 cm and 34 cm in core CJ06-435 is related to the formation of the YRD superlobe 1 and superlobe 10.

Compared with the pollen percentage, the pollen concentration can be interpreted in different ways. Namely, the percentage of different types of pollen is relative, whereas the pollen concentration is absolute, and it can directly reflect the amounts of pollen that were transported to the study area (Luo et al., 2013). It is crucial that a correct interpretation of pollen data is based on a percentage diagram as well as concentration. In core CJ06-435, the concentrations of herbs—especially *Chenopodiaceae* and *Artemisia* (Figure 7f)—were higher at depths of 160–94 cm (6570–5000 a BP) and 34–0 cm (after 1855 AD), except for the two sections of 160–135 cm and 34–19 cm. As mentioned in section 5.1, the extremely low pollen concentration in the sections of 160–135

cm and 34–19 cm was closely linked with the coarser sandy sediment. Combined with the results of pollen percentage and sediment grain size, we presumed that the higher herb pollen concentration in the periods of 6570–5000 a BP (160–94 cm) and after 1855 AD (34–0 cm) reflects changes in hydrographic conditions. Pollen data of surface sediments revealed that higher herb pollen concentrations occur in the YR, and the value of these concentrations showed a decreasing trend starting from the river mouth toward the ocean. The distribution pattern of surface pollen revealed that the YR is a major carrier for most herbs taxa in the sediment of Laizhou Bay (Yang et al., 2016). At the site of core CJ06-435, which is close to the mouth of the YR in Laizhou Bay, higher herb pollen concentrations in the Holocene samples may indicate increased fluvial discharge.

Sediment grain size provides direct information on changes of the sediment source and the sedimentary environment (Friedman and Sanders, 1978; Wu et al., 2015). The characteristics of grain size can be expressed by the grain size distribution curve, and usually the mean or median diameter is used (Xu, 1999). In this study, the value of mean grain size (Mz) showed that two major grain size boundaries occur at depths of 34 and 19 cm, separating a middle sedimentary unit (34–19 cm) that contains coarser sediment from the lower and upper sedimentary units that contain finer sediment (Figure 7d). The sand content of the upper, middle and lower layers was 11.2%, 33.6%, and 9%, respectively (Figure 7a); the silt content of these layers was 69%, 58.6%, and 76.1%, respectively (Figure 7b), and the clay content of these layers was 19.8%, 7.8%, and 14.8%, respectively (Figure 7c). On the basis of ^{137}Cs chronology (Figure 3), we speculate that these significant changes of grain size parameters at depths of 34 and 19 cm might represent a record of the channel shifts of the YR in 1855 AD and 1976 AD, respectively.

The sediment of Laizhou Bay mainly comes from the YR and other small rivers located in the southern part of Laizhou Bay (Zhang et al., 2017; Gao et al., 2018). Prior to 1855 AD, when the YR entered the Yellow Sea, the sediment contribution to the BS from other small rivers was relatively larger. The fine fraction suspension sediment that was derived from other small rivers favors the hypothesis of fine sediment accumulation in core CJ06-435 during this period.

When the YR reentered the BS after 1855 AD, the dispersal of YR material contributed substantially to the sedimentation of the BS. It was reported that more than 80% of the YR sediment discharges into the BS during the summer period (Bi et al., 2011). Owing to the barrier effect of the tidal shear front and the weak river flow, most of the river-delivered sediment is deposited on the

offshore delta within 15 km of the river mouth (Wang et al., 2007; Bi et al., 2010). Only a small part of the fine clay fraction is transported by the coastal currents over long distances and deposited across or along the shore in summer (Wu et al., 2015). During the winter (October to March) season, the much stronger winter monsoon generates large waves, resulting in intensive sediment resuspension in the coastal region owing to the enhanced bottom shear stress (Yang et al., 2011; Bi et al., 2011). The resuspended sediment is transported southeastward along the coast of Laizhou Bay by the monsoon-enhanced coastal currents passing through the location of the sediment core CJ06-435. Therefore, after 1855 AD, the sediment of core CJ06-435 mainly included the fine fraction of the suspended sediment dispersed from the YR mouth, the resuspended sediment from the coastal area off the YR delta in the winter, and the locally resuspended sediment.

The accumulation of YR-suspended sediment during the summer season in Laizhou Bay was closely associated with the sediment dispersion pattern off the active delta lobe (Xing et al., 2016). The estuary of the YR, during most of the period 1855–1976 AD, was north of the modern YRD, and suspended sediment from the YR was transported northeastward to Bohai Bay and the central Bohai basin. The contribution of YR-suspended sediment to the sedimentation of core CJ06-435 was smaller and the resuspended sediment became a dominant material source. During the winter, the large waves generated by the strong winds may result in intensive resuspension of the seabed sediment and lead to part of the coarse sediment in the YR mouth and Laizhou Bay being transported to the study area, which induces an evident increase in mean grain size and a decrease in the amount of fine sediment. After 1976 AD, the lower channel of the YR shifted to the Qingshuigou course in Laizhou Bay; the suspended sediments derived from the YR estuary were primarily driven southward and southeastward along the coast, leading an increasing transportation of most of the YR-suspended sediment into Laizhou Bay (Qiao et al., 2010). As a result, the dispersal of river-laden sediment contributed substantially to the sedimentation of core CJ06-435, with a fine sediment layer being formed in the upper part of the core.

The results inferred from our grain-size data on the migrations of the YR lower channel since 1855 AD and their effects on the sedimentary environments of the adjacent BS are in accordance with the results of other studies from Laizhou Bay (Wu et al., 2015) and central BS (Hu et al., 2011). Based on the records of sediment core collected from Laizhou Bay, Wu et al. (2015) found that when the YR mouth approached the core location, the sediment became finer; otherwise, the active

resuspension resulted in the accumulation of coarser sediment owing to strong hydrodynamics. The grain size results from the central mud areas of the BS also point to the conclusion that the sediment supply from the YR to the central BS was cut off because of the shift of the YR terminal course from the Diaokou source in outer Bohai Bay to the Qingshuigou course in Laizhou Bay in 1976; hence, resuspended sediment became a primary source of sediment dispersal in the central BS. As a result, there was a significant increase in the proportion of sand in surface sediment in the central BS (Hu et al., 2011).

It is worth noting that the variation of grain size characteristics in the period of 6570–5000 a BP is very similar to that after 1855 AD. As shown in Figure 7d, the shift of Mz in the period of 6570–5000 a BP also began with a significantly increased of Mz at 6570 a BP (160 cm) when the YR flowed into the BS in northern Shandong province. This similar variation of grain size in the period of 6570–5000 a BP (superlobe 1) and after 1855 AD (superlobe 10) implies that a similar YR channel shifting occurred during these two periods. However, further research is needed to reveal how the deltaic and neritic sea sedimentary environment was impacted by the river system.

5.3. Coastal salt marsh response to hydrological change

Two high-amplitude salt marsh vegetation shifts are displayed in the herb pollen record during 6570–5000 a BP (superlobe 1) and after 1855 AD (superlobe 10), indicating rapid oscillations of environmental conditions in the coastal area of BS. Within single intervals of the YR superlobe, a recurrent and directional alternation of herb pollen taxa is observed in the following order: the shift of herb pollen data began with an abrupt decrease of Cyperaceae pollen, followed by a steep increase of Chenopodiaceae and *Artemisia* pollen (Figure 8b).

Cyperaceae, Chenopodiaceae, and *Artemisia* are the three plant families/genus that contain the important representatives of coastal salt marsh plants (Lu et al., 2006). In the salt marsh of the modern YRD, species composition of Cyperaceae, Chenopodiaceae, and *Artemisia* varies with salinity and soil moisture. Plant families such as Cyperaceae are mainly composed of hydrophytes and phreatophyte *Eleocharis valleculosa*, *Cyperus rotundus*, *Scirpus planiculmis*, *S. triqueter*, *S. yagara*, *S. juncooides*, and *Juncellus serotinus* (Pan and Xu, 2011). The presence of Cyperaceae necessarily indicates lower saline conditions, since hydrophytes and phreatophyte sedges typically colonize in the middle and upper part of the supralittoral zone, both sides along the

riverbank, the coast of the lake, and the interfluvial lowlands of the paleo-river. These areas are far from the coastline, and the main type of soil is salinized soil with lower salinity (Zhang et al., 2009a; Xu, 2011). Chenopodiaceae are mainly composed of halophyte *Suaeda glauca*, *S. salsa*, and *Salicornia europaea*. *Artemisia* mainly consist of halophyte and xerophyte *Artemisia carvifolia*, *A. capillaris*, and *A. annua* (Xing et al., 2003; Zhang et al., 2009b). In the modern YRD, halophytes are distributed in the intertidal zone mudflat and the outside margin part of the supralittoral zone. These areas are near the coastline, characterized by a high incidence of wave brakes and prolonged inundation regimes, and the main type of soil is saline (Zhang et al., 2009b). Therefore, in salt marsh plant communities, the variation in the amount of Cyperaceae, Chenopodiaceae, and *Artemisia* is often thought to reflect environmental gradients controlled by the distance from the coast, local topography, terrigenous material, and freshwater input (González and Dupont, 2009; Zhang et al., 2009a). The pollen record from the BS could provide evidence of coastal salt marsh development over decades to centuries of the response to environmental alternations during the period of hydrological change.

In the studied sequence, the YR flowed into the BS toward the northern Shandong Province after a course shift. The lower river was initially braided upon relocation, as characterized by unchannelized river flow. At this initial stage, the river-derived sediment was largely accumulated in the floodplain and/or among the antecedent rivers owing to the lack of channelization (Wu et al., 2017), filling the coast of the lake, the interfluvial lowlands of the paleo-river, and the supralittoral zone, etc. This caused the destruction of hydrophytes and phreatophyte sedges in these areas. This process is indicated in our records by the significant decrease in the amount of Cyperaceae pollen percentages for superlobe 1 and superlobe 10 (Figure 8b).

Eventually, natural channel adjustments resulted in the coalescence of multiple channels into a single channel (Wu et al., 2017). A large amount of river-derived sediment was deposited at the mouth of the YR, causing the progradation of the YRD. Because of the strong influence of the tides, the intertidal zone in the YRD was originally bare beach. Along with the seaward expansion of the newly formed beach, the influence of tides was weakening on the original bare beach wetland and the salinity of the original beach wetland began to decrease (Zhang et al., 2007). Pioneer species of salt marshes, e.g., *Suaeda glauca*, *S. salsa* and *Salicornia europaea* (Chenopodiaceae), first colonized this original bare beach (Zhang et al., 2009a). The significant increase of Chenopodiaceae

in our pollen record (Figure 8b) is, therefore, interpreted as the development of the *S. glauca* population.

5.4. Palaeovegetation reconstruction and its climate significance

Based on the age model, the record between 3000 a BP and 1855 AD of core CJ06-435 is somewhat confused. Because the CSR was extremely low (about 0.005 cm/yr) during 3000 a BP to 1855 AD. As reported in recent studies, the CSR of cores from the tidal flat and neritic sea of the south BS were in the range 0.02–0.13 cm/yr before 2000 a BP (in cores H9601, H9602, ZK228, and ZK1, Figure 1; He et al., 2019), 0.04–0.06 cm/yr between 2000 a BP to 1855 AD (in cores ZK228, HB-1, and GYDY, Figure 1; He et al., 2019), and 0.35–1.38 cm/yr since 1855 AD (Wu et al., 2015; Qiao et al., 2017; Xu et al., 2018). Although core CJ06-435 is offshore compared to the other cores (e.g. H9601, H9602, ZK228, HB-1, ZK1 and GYDY), and it should have a lower CSR compared to those cores. But, the difference of CSR between CJ06-435 and those cores reach up to ten-fold. The reasonable explanation is that there might be some deposition hiatus between 3000 a BP and 1855 AD of core CJ06-435. The calculated CSR in the upper layer (since 1855 AD, as calculated to 0.17–0.48 cm/yr) and the lower layer (3000–8500 a BP, as calculated to 0.016–0.057 cm/yr) of core CJ06-435 are comparable to the nearby records by He et al. (2019) and Xu et al. (2018). Therefore, we just focused on the vegetation successions and climate change between 8500 and 3000 a BP, and only gave a cautious discussion for the chronology uncertain interval in this study.

During the period from 8500 to 6500 a BP (palynological zone 1, 271–156 cm), the palynofloral assemblages are mainly composed of the pollen of broadleaved trees, such as *Quercus*, *Betula*, *Alnus*, and *Ulmaceae*, combined with the pollen of hydrophytes and phreatophyte *Cyperaceae* and *Typha*; of these, the pollen of *Quercus* and *Typha* are predominant (Figures 4 and 5). In contrast, the pollen of halophytic and xerophytic herbs and conifer trees is scarce. The pollen assemblages encountered herein indicated that the vegetation of the BS land area consisted mainly of oak-rich temperate broadleaf deciduous forest, with some conifer trees on the uplands, and freshwater lakes and marshes dominating the coastal area, under the influence of a markedly warmer and wetter climate than the present. The highest values of AP pollen concentration (Figure 5), reflecting a dense vegetation cover, also represent warm conditions during this period. The pollen data are comparable to that found from previous palynological studies carried out in north China

(e.g., Yi et al., 2003; Ren, 2007; Chen and Wang, 2012; Li et al., 2019) and northeast China (e.g., Ren and Beug, 2002; Li et al., 2011; Stebich et al., 2015), from which a warm, wet climate corresponding to the Holocene Optimum was inferred. Under the influence of the Holocene Optimum, the forest cover evidently increased in north and northeast China (Ren, 2007). In the YR drainage area and Shandong Peninsula, the broadleaved deciduous forest thrived, accompanied by the presence of monsoonal evergreen forest and the abrupt decrease in the herbaceous taxa and conifers (Yi et al., 2003; Chen and Wang, 2012; Li et al., 2019).

During the period from 6500–5900 a BP (palynological zone 2a, 156–128 cm), a climatic cooling period is identified by an increase of conifers, *Pinus*, combined with an abrupt reduction of broadleaved trees (*Quercus*, *Betula*, *Alnus*, *Pterocarya*, Ulmaceae, and Moraceae). Halophytic and xerophytic herbs taxa such as Compositae, *Artemisia*, and Chenopodiaceae also increase, while Cyperaceae and aquatic herbs *Typha* obviously decreased. The climate shifted from warm, wet to cool, and dry may have caused the reduction of broadleaved deciduous forests, the expansion of conifer forests, and the gradually disappearance of freshwater lakes and marshes that had spread over the coastal area of BS. This result is in good agreement with previous studies. A pollen record from Shandong Peninsula revealed that *Quercus* content decreased, and herbs increased quickly following the Holocene Optimum, indicating a potential climate deterioration (Chen and Wang, 2012). A pollen record from Lake Bayanchagan in southern Inner Mongolia also showed that deciduous trees declined, conifers reached their maximum values, whilst steppe vegetation remained relatively high during 6500–5100 a BP, indicating cold and dry climate conditions (Jiang et al., 2006). It is worth noting that, a vast delta complex began to build up in the western part of the BS after 6570 a BP, which resulted in the increase of land area and development of the YR delta wetland. It can be concluded that the expansion of salt marsh during this period may be partly related to the formation of the YR delta complex.

During the period from 5900–3500 a BP (palynological zone 2b, 128–63 cm), climate cooling and drying is observed by a reduction of broadleaved trees such as *Quercus*, *Pterocarya*, Ulmaceae and Moraceae, and a rising frequency of halophytic and xerophytic herbs (*Artemisia* and Chenopodiaceae) (Figures 4 and 5). The cool, dry conditions probably cause the contraction of broadleaved forest and the expansion of halophytic and xerophytic herbs, which is similar to the findings of a study by Jiang et al. (2006). Based on the quantitative climatic reconstruction from

pollen and algal data for Lake Bayanchagan, Jiang et al. (2006) found that broadleaved trees, such as *Betula*, *Corylus*, *Ostryopsis* and *Ulmus* further declined, whereas the amount of steppe vegetation increased. The reconstruction of mean annual temperature and total annual precipitation dropped to their minimum values during 5100–2600 a BP.

Between 3500 and 3000 a BP (63–56 cm), a warm climatic phase occurred, as suggested by an increase in the amount of pollen from broadleaved trees (*Quercus*, *Betula*, *Alnus*, *Pterocarya*, and *Ulmaceae*), with low frequencies of conifer pollen (*Pinus*). Moreover, halophytic and xerophytic herb pollen, including *Compositae*, *Artemisia*, and *Chenopodiaceae*, were still present at a high frequency (Figures 4 and 5). Accordingly, the assemblages reveal that a warm, dry climate probably developed during this period.

From 3000 a BP to 1855 AD (56–30 cm), as mentioned in the first paragraph of this section, the CSR was extremely low during the period from 3000 a BP to 1855 AD (56–30 cm). We suggest that there might be some deposition hiatus and only tentatively discuss this section of the pollen record. This section begins with a relatively high percentage of broadleaved trees (*Quercus*, *Betula*, *Alnus*, *Pterocarya*, and *Ulmaceae*) and low frequencies of conifer pollen (*Pinus*) (56–41 cm); this is consistent with the previous stage (3500–3000 a BP, 63–56 cm). Afterward, there is a dramatic decrease in the occurrence of *Quercus*, quickly followed by a sudden increase in *Pinus* (41–30 cm, Figures 4 and 5). These pollen data suggest that the climate was warm during the latter part of this period (56–41 cm, 3000 a BP–?), following the climate condition of previous stage (63–56 cm, 3500–3000 a BP). In the earlier part of this period (41–30 cm, ?–1855 AD), the sudden increase in *Pinus* and major reductions of *Quercus* are likely signs of human impacts on the natural vegetation, including deforestation and cultivation. Park and Kim (2015) interpreted the decrease in the percentage of *Quercus* and increase of *Pinus* in the late Holocene as marking the development of secondary vegetation under anthropogenic influence. Based on two boreholes palynological from the YRD, Yi et al. (2003) found a sudden reduction of *Quercus*, followed by a marked increase of *Pinus* after 1300 a BP. Their research considered that this typical lag between the two taxa may indicate that, after the clearance of the local broadleaved deciduous forests, the vegetation was replaced by a secondary pine forest.

After 1855 AD (palynological zone 3, 30–0 cm), a significant decline in broadleaved trees (*Quercus*) and conifers (*Pinus*) pollen, as well as an increase in the frequency of herbs (*Poaceae*,

Compositae, *Artemisia*, and Chenopodiaceae) pollen may reflect the further strengthening of human disturbance on the vegetation and the expansion of intensive agricultural cultivation into forests of the BS coastal area. Moreover, after 1855 AD, the present YR began returning to the BS, and forming a vast area of floodplain and estuarine wetland on the southwest coast of the BS (Saito et al., 2000; Jiang et al., 2013). The variation of herb pollen may be partly related to the development of the modern YRD wetland.

5.5. Holocene temperature variations in north China and possible driving mechanisms

Many previous studies of north and northeast China have used the *Quercus* pollen percentage to infer regional temperature variation (Ren and Zhang, 1998; Yi et al., 2003; Li et al., 2004; Xu et al., 2014; Zhang et al., 2019). The *Quercus* pollen percentage from CJ06-435 core is consistent with previous studies, which also provide a regional air temperature reference. As shown in Figure 9d, the percentage of *Quercus* pollen in CJ06-435 core indicates a warm early Holocene from 8500 to 6500 a BP, a cool mid-Holocene from 6500 to 3500 a BP, and then a relatively warm late Holocene. These climate changes were also apparent in the change of *Quercus/Pinus* (Q/P) ratio. The average Q/P ratio was approximately 0.57 between 8500 and 6500 a BP, and changed to 0.33 between 6500 and 3500 a BP, and then gradually increased (Figure 9c).

The pollen-based record of temperature evolution from core CJ06-435 are broadly in-phase with published high-resolution sea surface temperature record from core YS01 (Figure 9e) of the Yellow Sea, suggesting at least a local pattern of temperature variations during the Holocene. To investigate whether the temperature pattern was local characteristics of the BS and Yellow Sea area, or whether it was rather a regional patterns of East Asia as a whole, the pollen records of core CJ06-435 were compared with recently-published and relatively well-dated sequences from north China, northwest China, and the Tibetan Plateau (see Figure 9a for site locations), including the sedimentary pollen-based temperature record from the Narenxia Peat within the Kanas Lake, Northwest China (Figure 9f; Feng et al., 2017); $U^{K_{37}}$ inferred temperature record at Lake Qinghai (Figure 9g; Hou et al., 2016); and lacustrine sedimentary pollen-based quantitative temperature record (the mean annual temperature) from Lake Bayanchagan in Inner Mongolia in north China (Figure 9h; Jiang et al., 2006). All three records indicate that the temperature was high between 8500 and 6000 a BP, low between 6000 and 4000–3000 a BP, and averagely high after 4000–3000

a BP (Figure 9f–h), this is consistent with the basic change pattern of our pollen-based temperature variation (Figure 9c and 9d). The comparison of the five records demonstrates that the CJ06-435 core *Quercus* pollen percentage record is, at a minimum, of regional significance.

Insolation has been widely accepted as an important factor in Holocene climate variation. The covariation of Northern Hemisphere extratropical (30 ° to 90 ° N) temperature and local summer insolation on an orbital scale, and the long-term decrease of summer insolation make the especially pronounced cooling of the Northern Hemisphere extra-tropics during the Holocene (Marcott et al., 2013) appear reasonable. However, the general pattern of temperature variation revealed by our study is not entirely consistent with local mean annual insolation forcing (Figure 9b). Our results indicated a cold mid-Holocene from 6500 to 3500 a BP and a relatively warm late Holocene. This temperature characterization of a cool mid-Holocene and a relatively warm late Holocene is also seen in many proxy records in the East Asia (Thompson et al., 1997; Jiang et al., 2006; Hou et al., 2016; Wu et al., 2016; Feng et al., 2017; Jia et al., 2019). The cooler mid-Holocene seen in the East Asia, could not solely be explained by the gradually decreasing summer insolation during the Holocene but might be related to other forcings.

We compared the pollen-based temperature record of core CJ06-435 (Figure 9c and 9d) with the frequency of El Niño events reconstructed from the Botryococcene concentration in the El Junco Lake sediment (Figure 9i; Zhang et al., 2014) and the ENSO variability reconstructed from $\delta^{18}\text{O}$ values of individual planktonic foraminifera retrieved from deep-sea sediments (Figure 9j; Koutavas and Joanides, 2012). As shown in Figure 9, lower temperature periods in the mid-Holocene tend to occur during a period of low El Niño activity, a relatively high temperature period in late Holocene tend to occur during a period of high El Niño activity, which indicates that there may be some link between the temperature of BS and Yellow Sea area and the ENSO system. Modern research suggests that ENSO can influence the evolution of temperature behavior, over interannual to multi-decadal time ranges (Hoerling et al., 2008; Triacca et al., 2014). In East Asia, many studies have indicated that the East Asian winter monsoon and the ENSO are tightly coupled (Zhou et al., 2007; Cheung et al., 2012; An et al., 2017). Generally, the strength of winter monsoon and East Asia troughs weakens in an El Niño year, and the weakening could cause the observed winter half-year warming (Xu et al., 2005). On centennial/millennial time scales, using pollen data from Lake Moon in the central part of the Great Khingan Mountain Range, Wu et al. (2019) recently connected

increased El Niño frequency with the decrease of winter monsoon activity in the East Asia, and the warming winter temperature in the Great Khingan Mountain Range since the mid-Holocene. Feng et al. (2017) founded that warm-phased ENSO was teleconnected with weakening of the Siberian High, and that the weakening was a cause of the observed winter half-year warming in southern Siberia. Likewise, the results of this study, indicating more or less synchronicity of the climate change in north China and ENSO activity, provide a possible linkage between the climate of north China and oceanic forcing during the mid-late Holocene.

In addition, radiative forcing by greenhouse gases (GHGs) rose 0.5 W/m^2 during the mid-late Holocene (Marcott et al., 2013), which would be expected to yield 1°C warming at Kinderlinskaya Cave in the southern Ural Mountains from 7000 a BP to the pre-industrial (Baker et al., 2017). Recently, both winter insolation and GHG forcing have been proposed as the major driving factors for winter warming during the Holocene in the Siberian Arctic (Meyer et al., 2015) and the southern Ural Mountains (Baker et al., 2017). Similarly, summer warming in central Asia during the mid-late Holocene, recorded by the alpine peat α -cellulose $\delta^{13}\text{C}$ record from the Altai Mountains (Rao et al., 2019), has been proposed to be mainly driven by the enhanced GHG forcing and increasing human activities. Rao et al. (2020) suggested that GHG forcing was the dominant driver of the summer and winter warming trends since ~5000 a BP. The effects of GHG forcing are global. Hence, we suggest that enhanced GHG forcing may be an important driver for mid-late Holocene temperature variations of East Asia.

In summary, the temperature characterizations of a cool mid-Holocene and a relatively warm late-Holocene revealed by the East Asia records could be linked with the change of insolation, ENSO activity and GHG forcing. The cooler mid-Holocene may be related to a combination of the decreasing summer insolation, weak El Niño activity, and relatively lower GHG radiative forcing during this interval. Along with strengthened ENSO activity and enhanced GHG forcing in the late Holocene, there was increased temperature.

6. Conclusions

Through the palynological and grain size reconstruction of coastal area vegetation and environment in core CJ06-435, we were able to identify specific responses of plant communities to climatic (temperature, precipitation), hydrological, and anthropogenic impacts. Our data elucidate

the pattern and mechanisms driving coastal salt marsh succession at decade-to-century timescales. Two intervals of expanded salt marsh vegetation correspond to the formation of YR delta superlobes, indicating that soil development and salinity gradients are the main factors determining the vegetation dynamics of coastal wetland. Our pollen-based temperature index revealed a warm early Holocene (8500–6500 a BP), a subsequent cool stage between 6500 and 3500 a BP, and a slightly warming episode after 3500 a BP. The reliability of the record, especially the cooler mid-Holocene, is further supported by several other temperature records from East Asia. We suggest that changes in insolation, ENSO activity and GHG forcing could have played an important role in the temperature evolution at the East Asia.

Code/Data availability

The co-authors declare that all data included in this study are available upon request by contact with the corresponding author (Email: jinxiachen@fio.org.cn).

Author contribution

Chen Jinxia wrote the manuscript; Shi Xuefa and Liu Yanguang revised the manuscript; Qiao Shuqing provided many constructive suggestions for the manuscript; Yang Shixiong provided the pollen data of surface sediment; Li Jianyong use pollen data of core CJ06-435 as base for quantitative climate reconstruction; Yan Shijuan, Lv Huahua, Li Xiaoyan and Li Chaoxin provided financial support for the collection of samples and obtained samples.

Competing interests

The authors declare that they have no conflict of interest.

Acknowledgements

We thank the crew of the R/V *Kan407* for sampling. We also thank Dr. Nan Qingyun for

improving this paper. This work was supported by the National Natural Science Foundation of China (Grant Nos. 41420104005 and 41576054).

References

- An, S.I., Kim, H.J., Park, W., Schneider, B.: Impact of ENSO on East Asian winter monsoon during interglacial periods: Effect of orbital forcing, *Clim. Dynam.*, 49, 3209–3219, 2017.
- Bao, R., Alonso, A., Delgado, C., Pagés, J.L.: Identification of the main driving mechanisms in the evolution of a small coastal wetland (Traba, Galicia, NW Spain) since its origin 5700 cal yr BP, *Palaeogeogr. Palaeoclimatol. Palaeoecol.*, 247, 296–312, 2007.
- Baker, J.L., Lachniet, M.S., Chervyatsova, O., Asmerom, Y., Polyak, V.: Holocene warming in western continental Eurasia driven by glacial retreat and greenhouse forcing, *Nat. Geosci.*, <https://doi.org/10.1038/NGEO2953>, 2017.
- Bi, N.S., Yang, Z.S., Wang, H.J., Hu, B.Q., Ji, Y.J.: Sediment dispersion pattern off the present Huanghe (Yellow River) subdelta and its dynamic mechanism during normal river discharge period, *Estuar. Coast. Shelf. S.*, 86, 352–362, 2010.
- Bi, N.S., Yang, Z.S., Wang, H.J., Fan, D.J., Sun, X.X., Lei, K.: Seasonal variation of suspended-sediment transport through the southern Bohai Strait, *Estuar. Coast. Shelf. S.*, 93, 239–247, 2011.
- Cheddadi, R., Rossignol-Strick, M.: Improved preservation of organic matter and pollen in Eastern Mediterranean sapropels, *Paleoceanography*, 10 (2), 301–309, 1995.
- Chen, J.X., Nan, Q.Y., Li, T.G., Sun, R.T., Sun, H.J., Lu, J.: Variations in the East Asian winter monsoon from 3500 to 1300 cal. yr BP in northern China and their possible societal impacts, *J. Asian. Earth. Sci.*, <https://doi.org/10.1016/j.jseas.2019.103912>, 2019a.
- Chen, J.X., Li, T.G., Nan, Q.Y., Shi, X.F., Liu, Y.G., Jiang, B., Zou, J.J., Selvaraj, K., Li, D.L., Li, C.S.: Mid-late Holocene rainfall variation in Taiwan: A high-resolution multiproxy record unravels the dual influence of the Asian monsoon and ENSO, *Palaeogeogr. Palaeoclimatol. Palaeoecol.*, 516, 139–151, 2019b.
- Chen, W., Wang, W.M.: Middle-Late Holocene vegetation history and environment changes revealed by pollen analysis of a core at Qingdao of Shandong Province, East China, *Quat. Int.*, 254, 68–72, 2012.
- Cheung, H.N., Zhou, W., Mok, H.Y., Wu, M.C.: Relationship between Ural-Siberian blocking and the East Asian winter monsoon in relation to the Arctic Oscillation and the El Niño–Southern Oscillation, *J. Climate*, 25(12), 4242–4257, 2012.
- Cohen, M.C.L., Lara, R.J., Smith, C.B., Angélica, R.S., Dias, B.S., Pequeno, T.: Wetland dynamics of Marajó Island, northern Brazil, during the last 1000 years, *Catena*, 76(1), 70–77, 2008.
- Cohen, M.C.L., Pessenda, L.C.R., Behling, H., Rossetti, D.d.F., França, M.C., Guimarães, J.T.F., Friaes, Y., Smith, C.B.: Holocene palaeoenvironmental history of the Amazonian mangrove belt, *Quat. Sci. Rev.*, 55, 50–58, 2012.
- Cui, B.S., Yang, Q.C., Yang, Z.F., Zhang, K.J.: Evaluating the ecological performance of wetland restoration in the Yellow River Delta, China, *Ecol. Eng.*, 35, 1090–1103, 2009.
- Dai, L., Weng, C.Y., Lu, J., Mao, L.M.: Pollen quantitative distribution in marine and fluvial surface

1689 sediments from the northern South China Sea: new insights into pollen transportation and deposition
1690 mechanisms, *Quat. Int.*, 325, 136–149, 2014.

1691 Dai, L., Weng, C.Y.: Marine palynological record for tropical climate variations since the late last glacial
1692 maximum in the northern South China Sea, *Deep-sea. Res. Pt. II.*, 122, 153–162, 2015.

1693 Engelhart, S.E., Horton, B.P., Roberts, D.H., Bryant, C.L., Corbett, D.R.: Mangrove pollen of Indonesia
1694 and its suitability as a sea-level indicator, *Mar. Geol.*, 242, 65–81, 2007.

1695 **Faegri, K., Iversen, J.: Textbook of Pollen Analysis, Alden Press, London, 370, 1992.**

1696 Feng, Z.D., Sun, A.Z., Abdusalih, N., Ran, M., Kurban, A., Lan, B., Zhang, D.L., Yang, Y.P.: Vegetation
1697 changes and associated climatic changes in the southern Altai Mountains within China during the
1698 Holocene, *Holocene*, 27(5), 683–693, 2017.

1699 França, M.C., Francisquini, M.I., Cohen, M.C.L., Pessenda, L.C.R., Rossetti, D.F., Guimarães, J.T.F.,
1700 Smith, C.B.: The last mangroves of Marajó Island–Eastern Amazon: Impact of climate and/or
1701 relative sea-level changes, *Rev. Palaeobot. Palyno.*, 187, 50–65, 2012.

1702 França, M.C., Alves, I.C.C., Castro, D.F., Cohen, M.C.L., Rossetti, D.F., Pessenda, L.C.R., Lorente, F.L.,
1703 Fontes, N.A., Junior, A.Á.B., Giannini, P.C.F., Francisquini, M.I.: A multi-proxy evidence for the
1704 transition from estuarine mangroves to deltaic freshwater marshes, Southeastern Brazil, due to
1705 climatic and sea-level changes during the late Holocene, *Catena*, 128, 155–166, 2015.

1706 Friedman, G.M., Sanders, J.E.: Principles of sedimentology, John Wiley and Sons, Inc, 1–792, 1978.

1707 Gao, M.S., Guo, F., Hou, G.H., Qiu, J.D., Kong, X.H., Liu, S., Huang, X.Y., Zhuang, H.H.: The evolution
1708 of sedimentary environment since late Pleistocene in Laizhou Bay, Bohai Sea, *Geol. Chin.*, 45(1),
1709 59–68, 2018. (in Chinese with English abstract)

1710 Giraldo-Giraldo, M.J., Velásquez-Ruiz, C.A., Pardo-Trujillo, A.: Late-Holocene pollen-based
1711 paleoenvironmental reconstruction of the El Triunfo wetland, Los Nevados National Park (Central
1712 Cordillera of Colombia), *Holocene*, 28(2), 183–194, 2018.

1713 González, C., Dupont, L.M.: Tropical salt marsh succession as sea-level indicator during Heinrich events,
1714 *Quat. Sci. Rev.*, 28, 939–946, 2009.

1715 **Grimm, E.C.: CONISS: a Fortran 77 program for stratigraphically constrained cluster analysis by the**
1716 **method of incremental sum of squares. *Comput. Geosci.*, 13, 13–35, 1987.**

1717 Gu, Y.H., Xiu, R.C.: On the current and storm flow in the Bohai Sea and their role in transporting
1718 deposited silt of the Yellow River, *J. Oceanogr. Huanghai & Bohai Seas.*, 14(1), 1–6, 1996.

1719 Hao, T., Liu, X.J., Ogg, J., Liang, Z., Xiang, R., Zhang, X.D., Zhang, D.H., Zhang, C., Liu, Q.L., Li,
1720 X.G.: Intensified episodes of East Asian Winter Monsoon during the middle through late Holocene
1721 driven by North Atlantic cooling events: High-resolution lignin records from the South Yellow Sea,
1722 China, *Earth. Planet. Sci. Lett.*, 479, 144–155, 2017.

1723 **Havinga, A.J.: Palynology and pollen preservation, *Rev. Palaeobot. Palyno.*, 2, 81–98, 1967.**

1724 He, L., Xue, C.T., Ye, S.Y., Amorosi, A., Yuan, H.M., Yang, S.X., Laws, E.A.: New evidence on the
1725 spatial-temporal distribution of superlobes in the Yellow River Delta Complex, *Quat. Sci. Rev.*, 214,
1726 117–138, 2019.

1727 Hemavathi, S., Manjula, R., Ponmani, N.: Numerical Modelling and Experimental Investigation on the
1728 Effect of Wave Attenuation Due to Coastal Vegetation, *Proceedings of the Fourth International*
1729 *Conference in Ocean Engineering (ICOE2018)*, 23, 99–110, 2019.

1730 Hendy, I.L., Minckley, T.A., Whitlock, C.: Eastern tropical Pacific vegetation response to rapid climate
1731 change and sea level rise: A new pollen record from the Gulf of Tehuantepec, southern Mexico,
1732 *Quat. Sci. Rev.*, 145, 152–160, 2016.

1733 Heusser, L.E.: Pollen distribution in marine sediments on the continental margin off northern California.
1734 *Mar. Geol.*, 80, 131–147, 1988.

1735 Hoerling, M., Kumar, A., Eischeid, J., Jha, B.: What is causing the variability in global mean land
1736 temperature?, *Geophys. Res. Lett.*, 35, L23712, 2008.

1737 Hou, X.Y.: *Vegetation Atlas of China*, Science Press, 1–280, 2001. (in Chinese)

1738 Hou, J.Z., Huang, Y.S., Zhao, J.T., Liu, Z.H., Colman, S., An, Z.S.: Large Holocene summer temperature
1739 oscillations and impact on the peopling of the northeastern Tibetan Plateau, *Geophys. Res. Lett.*, 43,
1740 1323–1330, 2016.

1741 Hu, L.M., Guo, Z.G., Shi, X.F., Qin, Y.W., Lei, K., Zhang, G.: Temporal trends of aliphatic and
1742 polyaromatic hydrocarbons in the Bohai Sea, China: Evidence from the sedimentary record, *Org.*
1743 *Geochem.*, 42, 1181–1193, 2011.

1744 Huang, D.J., Su, J.L., Backhaus, J.O.: Modelling the seasonal thermal stratification and baroclinic
1745 circulation in the Bohai Sea, *Cont. Shelf. Res.*, 19, 1485–1505, 1999.

1746 Jia, Y.H., Li, D.W., Yu, M., Zhao, X.C., Xiang, R., Li, G.X., Zhang, H.L., Zhao, M.X.: High- and low-
1747 latitude forcing on the south Yellow Sea surface water temperature variations during the Holocene,
1748 *Global. Planet. Change.*, 182, 103025, 2019.

1749 Jiang, W.Y., Guo, Z.T., Sun, X.J., Wu, H.B., Chu, G.Q., Yuan, B.Y., Hatte, C., Guiot, J.: Reconstruction
1750 of climate and vegetation changes of Lake Bayanchagan (Inner Mongolia): Holocene variability of
1751 the east Asian monsoon, *Quat. Res.*, 65, 411–420, 2006.

1752 Jiang, D.J., Fu, X.F., Wang, K.: Vegetation dynamics and their response to freshwater inflow and climate
1753 variables in the Yellow River Delta, China, *Quat. Int.*, 304, 75–84, 2013.

1754 Kirchner, G., Ehlers, H.: Sediment Geochronology in Changing Coastal Environments: Potentials and
1755 Limitations of the ¹³⁷Cs and ²¹⁰Pb Methods, *J. Coast. Res.*, 14, 483–492, 1998.

1756 Koutavas, A., Joanides, S.: El Niño–Southern Oscillation extrema in the Holocene and Last Glacial
1757 Maximum, *Paleoceanography*, <https://doi.org/10.1029/2012PA002378>, 2012.

1758 Li, C.Y., Yan, L.Q., Han, T.X.: Research on composition of wetland vegetation in Shandong, Shandong
1759 Forest Sci. Tech., 4, 27–29, 2007. (in Chinese with English abstract)

1760 Li, X.Q., Zhou, J., Shen, J., Weng, C.Y., Zhao, H.L., Sun, Q.L.: Vegetation history and climatic variations
1761 during the last 14 ka BP inferred from a pollen record at Daihai Lake, north-central China, *Rev.*
1762 *Palaeobot. Palyno.*, 132, 195–205, 2004.

1763 Li, C.H., Wu, Y.H., Hou, X.H.: Holocene vegetation and climate in Northeast China revealed from Jingbo
1764 Lake sediment, *Quat. Int.*, 229, 67–73, 2011.

1765 Li, G.G., Hu, B.Q., Bi, J.Q., Song, Z.L., Bu, R.Y., Li, J.M.: Stratigraphic evolution of the Huanghe Delta
1766 (Bohai Sea) since the Late Quaternary and its paleoenvironmental implications: evidence from core
1767 ZK1, *Acta Sedimentol. Sin.*, 31 (6), 1050–1058, 2013. (in Chinese with English abstract)

1768 Li, M.Y., Zhang, S.R., Xu, Q.H., Xiao, J., Wen, R.L.: Spatial patterns of vegetation and climate in the
1769 North China Plain during the Last Glacial Maximum and Holocene climatic optimum, *Sci. China.*
1770 *Earth. Sci.*, 62 (8), 1279–1287, 2019.

1771 Liu, J., Saito, Y., Wang, H., Zhou, L., Yang, Z.: Stratigraphic development during the Late Pleistocene
1772 and Holocene offshore of the Yellow River delta, Bohai Sea, *J. Asian. Earth. Sci.*, 36, 318–331,
1773 2009a.

1774 Liu, W.Z., Zhang, Q.F., Liu, G.H.: Seed banks of a river–reservoir wetland system and their implications
1775 for vegetation development, *Aquat. Bot.*, 90, 7–12, 2009b.

1776 Liu, S., Feng, A., Du, J., Xia, D., Li, P., Xue, Z., Hu, W., Yu, X.: Evolution of the buried channel systems

1777 under the modern Yellow River delta since the last glacial maximum, *Quat. Int.*, 349, 327–338, 2014.

1778 Liu, D.Y., Li, X., Emeis, K.C., Wang, Y.J., Richard, P.: Distribution and sources of organic matter in
1779 surface sediments of Bohai Sea near the Yellow River Estuary, China, *Estuar. Coast. Shelf. S.*, 165,
1780 128–136, 2015.

1781 Lu, J.J., He, W.S., Tong, C.F., Wang, W.: *Wetland Ecology*. Higher Education Press, Beijing, 2006.

1782 Luo, C.X., Chen, M.H., Xiang, R., Liu, J.G., Zhang, L.L., Lu, J., Yang, M.X.: Characteristics of modern
1783 pollen distribution in surface sediment samples for the northern South China Sea from three
1784 transects, *Quat. Int.*, 286, 148–158, 2013.

1785 Luo, C.X., Chen, M.H., Xiang, R., Liu, J.G., Zhang, L.L., Lu, J., Yang, M.X.: Modern pollen distribution
1786 in marine sediments from the northern part of the South China Sea, *Mar. Micropaleontol.*, 108, 41–
1787 56, 2014.

1788 Marcott, S.A., Shakun, J.D., Clark, P.U., Mix, A.C.: A reconstruction of regional and global temperature
1789 for the past 11,300 years, *Science*, 339, 1198–1201, 2013.

1790 Meyer, H., Opel, T., Laepple, T., Dereviagin, A.Y., Hoffmann, K., Werner, M.: Long-term winter
1791 warming trend in the Siberian Arctic during the mid- to late Holocene, *Nat. Geosci.*, [https://doi.org/](https://doi.org/10.1038/NGEO2349)
1792 10.1038/NGEO2349, 2015.

1793 Milliman, J.D., Meade, R.H.: World-wide delivery of river sediment to oceans, *J. Geol.*, 91, 1–21, 1983.

1794 Milliman, J.D., Qin, Y.S., Ren, M.E., Saito, Y.: Man's influence on the erosion and transport of sediment
1795 by Asian rivers: the Yellow River (Huanghe) example, *J. Geol.*, 95, 751–762, 1987.

1796 Montade, V., Nebout, N.C., Kissel, C., Mulsow, S.: Pollen distribution in marine surface sediments from
1797 Chilean Patagonia, *Mar. Geol.*, 282, 161–168, 2011.

1798 Mudie, P.J.: Pollen distribution in recent marine sediments, Eastern Canada, *Can. J. Earth Sci.*, 19, 729–
1799 747, 1982.

1800 Mudie, P.J., Mc Carthy, F.M.G.: Pollen transport processes in the western North Atlantic: evidence from
1801 cross margin and north–south transects, *Mar. Geol.*, 118, 79–105, 1994.

1802 Neumann, F.H., Scott, L., Bousman, C.B., As, L.V.: A Holocene sequence of vegetation change at Lake
1803 Eteza, coastal KwaZulu-Natal, South Africa, *Rev. Palaeobot. Palyno.*, 162, 39–53, 2010.

1804 Pan, Y., Xu, J.W.: Studies on Resource and Flora of Aquatic Vascular Plants in Wetland of Yellow River
1805 Delta, *J. Anhui. Agr. Sci.*, 39(3), 1642–1644, 2011. (in Chinese with English abstract)

1806 Palinkas, C.M., Nittrouer, C.A.: Modern sediment accumulation on the Po shelf, Adriatic Sea, *Cont.*
1807 *Shelf. Res.*, 27, 489–505, 2007.

1808 Park, J., Kim, M.: Pollen-inferred late Holocene agricultural developments in the vicinity of Woljeong-
1809 ri, southwestern Korea, *Quat. Int.*, 384, 13–21, 2015.

1810 Pessenda, L.C.R., Vidotto, E., Oliveira, P.E.D., Jr, A.A.B., Cohen, M.C.L., Rossetti, D.d.F., Ricardi-
1811 Branco, F., Bendassolli, J.A.: Late Quaternary vegetation and coastal environmental changes at Ilha
1812 do Cardoso mangrove, southeastern Brazil, *Palaeogeogr. Palaeoclimatol. Palaeoecol.*, 363–364, 57–
1813 68, 2012.

1814 Qiao, F.L., Gan, Z.J., Sun, X.P.: *Regional oceanography of China seas-physical oceanography*, China.
1815 *Ocean. Press.*, 2012.

1816 Qiao, S.Q., Shi, X.F., Zhu, A.M., Liu, Y.G., Bi N.S., Fang, X.S., Yang, G.: Distribution and transport of
1817 suspended sediments off the Yellow River (Huanghe) mouth and the nearby Bohai Sea, *Estuar. Coast.*
1818 *Shelf. S.*, 86, 337–344, 2010.

1819 Qiao, S.Q., Shi, X.F., Wang, G.Q., Zhou, L., Hu, B.Q., Hu, L.M., Yang, G., Liu, Y.G., Yao, Z.Q., Liu,
1820 S.F.: Sediment accumulation and budget in the Bohai Sea, Yellow Sea and East China Sea, *Mar.*

1821 Geol., 390, 270–281, 2017.

1822 Rao, Z.G., Huang, C., Xie, L.H., Shi, F.X., Zhao, Y., Cao, J.T., Gou, X.H., Chen, J.H., Chen, F.H.: Long-
1823 term summer warming trend during the Holocene in central Asia indicated by alpine peat α -cellulose
1824 $\delta^{13}\text{C}$ record, Quat. Sci. Rev., 203, 56–67, 2019.

1825 Rao, Z.G., Shi, F.X., Li, Y.X., Huang, C., Zhang, X.Z., Yang, W., Liu, L.D., Zhang, X.P., Wu, Y.: Long-
1826 term winter/summer warming trends during the Holocene revealed by α -cellulose $\text{d18O}/\text{d13C}$
1827 records from an alpine peat core from central Asia. Quat. Sci. Rev., 232, 106217, 2020.

1828 Ren, G.Y., Zhang, L.S.: A preliminary mapped summary of Holocene pollen data for northeast China,
1829 Quat. Sci. Rev., 17, 669–688, 1998.

1830 Ren, G.Y., Beug, H.J.: Mapping Holocene pollen data and vegetation of China, Quat. Sci. Rev., 21, 1395–
1831 1422, 2002.

1832 Saito, Y., Wei, H.L., Zhou, Y.Q., Nishimura, A., Sato, Y., Yokota, S.: Delta progradation and chenier
1833 formation in the Huanghe (Yellow River) delta, China, J. Asian. Earth. Sci., 18, 489–497, 2000.

1834 Sander, V.D.K.: Pollen distribution in marine sediments from the south-eastern Indonesian waters,
1835 Palaeogeogr. Palaeoclimatol. Palaeoecol., 171, 341–361, 2001.

1836 Serrano, O., Lovelock, C.E., Atwood, T.B., Macreadie, P.I., Canto, R., Phinn, S., Arias-Ortiz, A., Bai, L.,
1837 Baldock, J., Bedulli, C., et al.: Australian vegetated coastal ecosystems as global hotspots for climate
1838 change mitigation, Nat. Commun., <https://doi.org/10.1038/s41467-019-12176-8>, 2019.

1839 Spivak, A.C., Sanderman, J., Bowen, J.L., Canuel, E.A., Hopkinson, C.S.: Global-change controls on
1840 soil-carbon accumulation and loss in coastal vegetated ecosystems, Nat. Geosci., 12, 685–692, 2019.

1841 Stebich, M., Rehfeld, K., Schlütz, F., Tarasov, P.E., Liu, J.Q., Mingram, J.: Holocene vegetation and
1842 climate dynamics of NE China based on the pollen record from Sihailongwan Maar Lake, Quat. Sci.
1843 Rev., 124, 275–289, 2015.

1844 Stuiver, M., Reimer, P.J., Reimer, R.W.: CALIB 7.1 [WWW program, <http://calib.org>], 2019.

1845 Thompson, L.G., Yao, T.D., Davis, M.E., Henderson, K.A., Mosley-Thompson, E., Lin, P.N., Beer, J.,
1846 Synal, H.A., Cole-Dai, J., Bolzan, J.F.: Tropical climate instability: the last glacial cycle from a
1847 Qinghai-Tibetan ice core, Science, 276, 1821–1825, 1997.

1848 Triacca, U., Pasini, A., Attanasio, A., Giovannelli, A., Lippi, M.: Clarifying the Roles of Greenhouse
1849 Gases and ENSO in Recent Global Warming through Their Prediction Performance, J. Clim., 27,
1850 7903–7910, 2014.

1851 Wang, K.F. and others: Spore-pollen and algal assemblages in the sediments of the Bohai Sea and
1852 palaeoenvironments, Geological Publishing House, Beijing, 1993.

1853 Wang, H., Yang, Z., Li, Y., Guo, Z., Sun, X., Wang, Y.: Dispersal pattern of suspended sediment in the
1854 shear frontal zone off the Huanghe (Yellow River) mouth, Cont. Shelf. Res., 27, 854–871, 2007.

1855 Wang, H.J., Wang, A.M., Bi, N.S., Zeng, X.M., Xiao, H.H.: Seasonal distribution of suspended sediment
1856 in the Bohai Sea, China, Cont. Shelf. Res., 90, 17–32, 2014.

1857 Woodroffe, S.A., Long, A.J., Milne, G.A., Bryant, C.L., Thomas, A.L.: New constraints on late Holocene
1858 eustatic sea-level changes from Mahe, Seychelles, Quat. Sci. Rev., 115, 1–16, 2015.

1859 Wu, X., Bi, N.S., Kanai, Y., Saito, Y., Zhang, Y., Yang, Z.S., Fan, D.J., Wang, H.J.: Sedimentary records
1860 off the modern Huanghe (Yellow River) delta and their response to deltaic river channel shifts over
1861 the last 200 years, J. Asian. Earth. Sci., 108, 68–80, 2015.

1862 Wu, P., Xiao, X., Tao, S., Yang, Z., Zhang, H., Li, L., Zhao, M.: Biomarker evidence for changes in
1863 terrestrial organic matter input into the Yellow Sea mud area during the Holocene, Sci. China. Earth.
1864 Sci., 59, 1216–1224, 2016.

1865 Wu, X., Bi, N.S., Xu, J.P., Nitttrouer, J.A., Yang, Z.S., Saito, Y., Wang, H.J.: Stepwise morphological
1866 evolution of the active Yellow River (Huanghe) delta lobe (1976–2013): Dominant roles of riverine
1867 discharge and sediment grain size, *Geomorphology*, [https://doi.org/10.1016/](https://doi.org/10.1016/j.geomorph.2017.04.042)
1868 [j.geomorph.2017.04.042](https://doi.org/10.1016/j.geomorph.2017.04.042), 2017.

1869 Wu, J., Liu, Q., Cui, Q. Y., Xu, D. K., Wang, L., Shen, C. M., Chu, G.Q., Liu, J.Q.: Shrinkage of East
1870 Asia winter monsoon associated with increased ENSO events since the mid-Holocene, *J. Geophys.*
1871 *Res.*, 124, 3839–3848, 2019.

1872 Xing, S.Y., Xi, J.B., Zhang, J.F., Song, Y.M., Ma, B.Y.: The basic characteristics and the main types of
1873 vegetation in the Yellow River delta region, *J. Northeast. Forest. Univ.*, 31(6), 85–86, 2003. (in
1874 Chinese)

1875 Xing, G.P., Wang, H.J., Yang, Z.S., Bi, N.S.: Spatial and temporal variation in erosion and accumulation
1876 of the subaqueous Yellow River delta (1976–2004), *J. Coast. Res.*, 74, 32–47, 2016.

1877 Xu, J.X.: Grain-size characteristics of suspended sediment in the Yellow River, China, *Catena*, 38, 243–
1878 263, 1999.

1879 Xu, W.C., Ma, J.s., Wang, W.: A review of studys on the influence of ENSO events on the climate in
1880 China, *Sci. Meteorol. Sin.*, 25(2), 212–220, 2005.

1881 Xu, J.W.: Research on Diversity of Aquatic Vascular Plants in Wetland of Yellow River Delta,
1882 Heilongjiang. *Agr. Sci.*, 1, 36–38, 2011. (in Chinese with English abstract)

1883 Xu, D.K., Lu, H.Y., Chu, G.Q., Wu, N.Q., Shen, C.M., Wang, C., Mao, L.M.: 500-year climate cycles
1884 stacking of recent centennial warming documented in an East Asian pollen record, *Sci. Rep-UK.*, 4,
1885 3611, 2014.

1886 Xu, Y.P., Zhou, S.Z., Hu, L.M., Wang, Y.H., Xiao, W.J.: Different controls on sedimentary organic carbon
1887 in the Bohai Sea: River mouth relocation, turbidity and eutrophication. *J. Marine. Syst.*, 180, 1–8,
1888 2018.

1889 Xu, Z.J., Zhang, X.L., Zhang, Z.H., Zhang, W.: Analysis of the biodiversity characters of coastal wetlands
1890 in southern Laizhou Bay, *Ecol. Env. Sci.*, 19(2), 367–372, 2010. (in Chinese with English abstract)

1891 Xue, C., Cheng, G.D., Zhou, Y.Q.: Relationship between Late Pleistocene and Early Holocene terrestrial
1892 deposits and sea level changes in Yellow River Delta area. *Mar. Geol. Quat. Geol.*, 8 (2), 63–73,
1893 1988. (in Chinese with English abstract)

1894 Xue, C.T., Cheng, G.D.: Shelly ridges in west coast of Bohai Sea and Holocene Yellow River Delta
1895 system. In: Yang, Z.G., Lin, H.M. (Eds.), *Quaternary Processes and Events in China Offshore and*
1896 *Onshore Areas, China. Ocean. Press.*, 1989. (in Chinese with English abstract)

1897 Xue, C.T.: Historical changes in the Yellow River delta, China, *Mar. Geol.*, 113, 321–329, 1993.

1898 Xue, C.T., Zhu, X.H., Lin, H.M.: Holocene sedimentary sequence, foraminifera and ostracoda in west
1899 coastal lowland of Bohai Sea, China, *Quat. Sci. Rev.*, 14, 521–530, 1995.

1900 Yang, Z.S., Ji, Y.J., Bi, N.S., Lei, K., Wang, H.J.: Sediment transport off the Huanghe (Yellow River)
1901 delta and in the adjacent Bohai Sea in winter and seasonal comparison, *Estuar. Coast. Shelf. S.*, 93,
1902 173–181, 2011.

1903 Yang, S.X., Li, J., Mao, L.M., Liu, K., Gao, M.S., Ye, S.Y., Yi, S., Zhou, L.Y., Wang, F.F.: Assessing
1904 pollen distribution patterns and provenance based on palynological investigation on surface
1905 sediments from Laizhou Bay, China: an aid to palaeoecological interpretation, *Palaeogeogr.*
1906 *Palaeoclimatol. Palaeoecol.*, 457, 209–220, 2016.

1907 Yang, S.X., Song, B., Ye, S.Y., Laws, E.A., He, L., Li, J., Chen, J.X., Zhao, G.M., Zhao, J.T., Mei, X.,
1908 Behling, H.: Large-scale pollen distribution in marine surface sediments from the Bohai Sea, China:

- Insights into pollen provenance, transport, deposition, and coastal-shelf paleoenvironment, *Prog. Oceanog.*, 178, 102183, 2019.
- Yi, S., Saito, Y., Oshima, H., Zhou, Y.Q., Wei, H.L.: Holocene environmental history inferred from pollen assemblages in the Huanghe (Yellow River) delta, China: climatic change and human impact, *Quat. Sci. Rev.*, 22, 609–628, 2003.
- Zhang, G.S., Wang, R.Q., Song, B.M.: Plant community succession in modern Yellow River Delta, China, *J. Zhejiang Univ. Sci.*, 8(8), 540–548, 2007.
- Zhang, X.L., Ye, S.Y., Yin, P., Chen, D.J.: Characters and successions of natural wetland vegetation in Yellow River Delta, *Ecol. Env. Sci.*, 18(1), 292–298, 2009a. (in Chinese with English abstract)
- Zhang, X.L., Ye, S.Y., Yin, P., Yuan, H.M.: Flora characteristics of vascular plants of coastal wetlands in Yellow River Delta, *Ecol. Env. Sci.*, 18(2), 600–607, 2009b. (in Chinese with English abstract)
- Zhang, Z.H., Leduc, G., Sachs, J.P.: El Niño evolution during the Holocene revealed by a biomarker rain gauge in the Gal ápagos Islands, *Earth Planet. Sci. Lett.*, 404, 420–434, 2014.
- Zhang, P., Hu, R.J., Zhu, L.H., Wang, P., Yin, D.X., Zhang, L.J.: Distributions and contamination assessment of heavy metals in the surface sediments of western Laizhou Bay: Implications for the sources and influencing factors, *Mar. Pollut. Bull.*, <https://doi.org/10.1016/j.marpolbul.2017.03.046>, 2017.
- Zhang, H.X., Zhang, M.L., Xu, T.P., Tang, J.: Numerical Investigations of Tsunami Run-Up and Flow Structure on Coastal Vegetated Beaches, *Water*, <https://doi.org/10.3390/w10121776>, 2018.
- Zhang, J.Y., Li, J., Yan, Y., Li, J.J., Wan, X.Q.: A 1000-year record of centennial-scale cyclical vegetation change from Maar Lake Sanjiaolongwan in northeastern China, *J. Asian. Earth. Sci.*, 176, 315–324, 2019.
- Zheng, Z., Yang, S.X., Deng, Y., Huang, K.Y., Wei, J.H., Berne, S., Suc, J.P.: Pollen record of the past 60 ka BP in the Middle Okinawa Trough: Terrestrial provenance and reconstruction of the paleoenvironment, *Palaeogeogr. Palaeoclimatol. Palaeoecol.*, 307, 285–300, 2011.
- Zhou, L.Y., Liu, J., Saito, Y., Gao, M.S., Diao, S.B., Qiu, J.D., Pei, S.F.: Modern sediment characteristics and accumulation rates from the delta front to prodelta of the Yellow River (Huanghe), *Geo-Mar. Lett.*, 36, 247–258, 2016.
- Zhou, W., Wang, X., Zhou, T.J., Li, C., Chan, J.C.L.: Interdecadal variability of the relationship between the East Asian winter monsoon and ENSO, *Meteorol. Atmos. Phys.*, 98, 283–293, 2007.
- Zhou, Z., Bian, C., Wang, C., Jiang, W., Bi, R.: Quantitative assessment on multiple timescale features and dynamics of sea surface suspended sediment concentration using remote sensing data, *J. Geophys. Res-Oceans.*, 122, 8739–8752, 2017.

1950 **Table captions**

1951

1952 **Table 1**

1953 AMS radiocarbon dates from core CJ06-435 and one tie points corresponding to the deepest onset of

1954 ¹³⁷Cs in environmental samples at measurable levels; for calibration in years before present (a BP) 0 =

1955 1950 AD.

1956

Core depth (cm)	Materials	Radiocarbon date (a)	Age error (a)	Calibrated age (1σ) (a BP)	Mean calibrated age (a BP)	Laboratory
25	¹³⁷ Cs	–	–	–	–4	NIGLAS
7	Mixed benthic foraminifera	3020	30	2854-3039	2951	Beta
13	Mixed benthic foraminifera	2990	30	2817-2997	2913	Beta
17	Mixed benthic foraminifera	3060	30	2908-3102	3003	WHOI
59	Mixed benthic foraminifera	3340	30	3270-3485	3359	Beta
69	Mixed benthic foraminifera	3590	25	3563-3725	3656	WHOI
87	Mixed benthic foraminifera	4450	30	4695-4878	4801	Beta
119	Mixed benthic foraminifera	5200	30	5604-5770	5706	WHOI
129	Mixed benthic foraminifera	4520	30	4812-4965	4894	Beta
161	Mixed benthic foraminifera	6020	30	6501-6667	6592	WHOI
183	Mixed benthic foraminifera	6340	35	6886-7081	6981	WHOI

1957

1958

1959

1960

1961

1962

1963

1964

1965

1966

1967

1968

1969

1970

1971

1972

1973

Figure caption

Figure 1: Geographic map of the Bohai Sea, with locations of core CJ06-435 (red circle) and other sites referred to in this study (purple circles). Cores references: H9601 and H9602 (Saito et al., 2000), ZK1 (Li et al., 2013), ZK228 (Xue et al., 1988), HB-1 (Liu et al., 2009a), GYDY (Liu et al., 2014).

Figure 2: Vegetation map around the Bohai Sea and the ocean current in the Bohai Sea during the summer (a) and winter (b) (YSWC: Yellow Sea Warm Current; SBSCC: Southern Bohai Sea Coastal Current; LNCC: Liaonan Coastal Current; LBCC: Lubei Coastal Current, modified from Qiao et al., 2010; the vegetation dataset was provided by the Environmental and Ecological Science Data Center for West China, National Natural Science Foundation of China [<http://westdc.westgis.ac.cn>] and is based on the Vegetation Atlas of China, 1:1000,000; Hou, 2001).

Figure 3: Lithology, grain size, color reflectance L^* and a^* , magnetic susceptibility, and activity profiles for ^{137}Cs and ^{210}Pb of core CJ06-435.

Figure 4: Percentage diagram of the principal pollen taxa from core CJ06-435. Pollen zonation is based on CONISS results.

Figure 5: Concentration diagram of the principal pollen taxa from core CJ06-435.

Figure 6: Spatial distribution of modern pollen percentage (black solid circle, %) and concentration (red open circle, grains/g) in Laizhou Bay, Bohai Sea (modified from Yang et al., 2016).

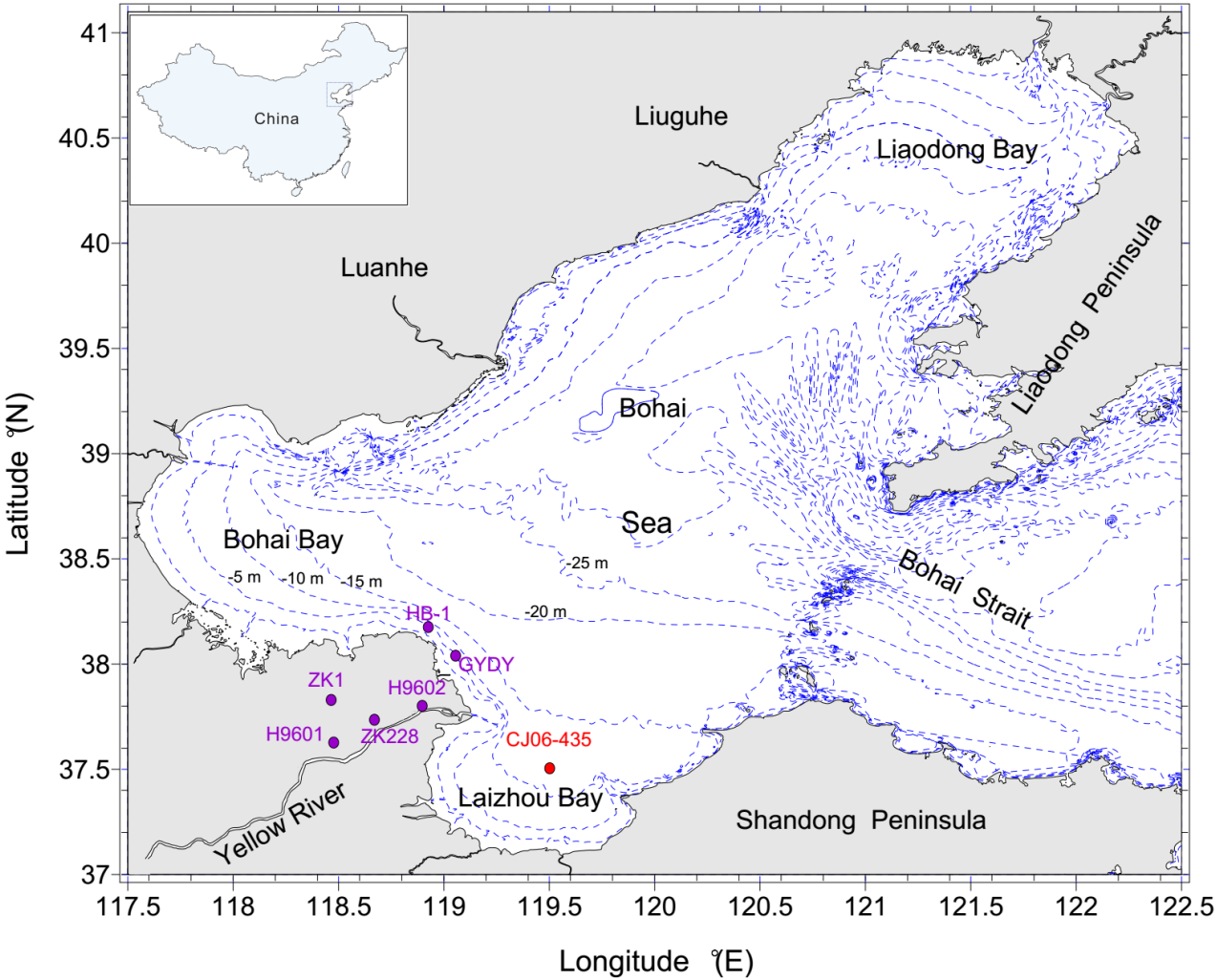
Figure 7: (a-f) Vertical profiles of grain-size parameters and halophytic and xerophytic herb (Chenopodiaceae and *Artemisia*) pollen percentage and concentration of core CJ06-435 (Mz – mean grain size). (g) The location of Yellow River superlobe 1 (Lijin superlobe) and superlobe 10 (Modern superlobe) (modified after Xue, 1993).

Figure 8: (a) Correlating proxy to paleo-superlobe variation of the YR, from top to bottom: percentage of Cyperaceae, Chenopodiaceae, and *Artemisia* pollen; concentration of Chenopodiaceae, *Artemisia*, and Cyperaceae pollen; sand percentage. (b) Detailed pollen and grain size profiles representing salt marsh species (Cyperaceae, Chenopodiaceae, *Artemisia*) relative abundances and hydrodynamic change during the formation of Yellow River superlobe 1 and 10. Pollen percentage of Cyperaceae, Chenopodiaceae and *Artemisia* from core CJ06-435 indicating the directional alternation of salt marshes along the Bohai Sea, ①— Unchannelized river flow characterized the onset of Yellow River channel shift, caused a large amount of river-derived sediment accumulation in the floodplain and destroyed the sedges in the coastal depression; ②

—Along with the formation of a new channel, lateral migration of the lower channel stopped, and new intertidal mudflat was formed. Pioneer species (*Chenopodiaceae*, *Artemisia*) first colonize bare zones of lower and middle marsh areas.

Figure 9: Comparison of relevant Holocene temperature records with solar irradiance and ENSO proxy records derived from the equatorial Pacific. (a) Locations of the sites where the Holocene temperature records are derived. The schematic large-scale diagram modified from Hao et al. (2017). In the diagram, the purple area is Tibetan Plateau, the yellow area is Chinese Loess Plateau, and numbered dots refer to the corresponding study sites. (b) Summer (mean of June) insolation irradiance for the Northern Hemisphere (40°N). (c,d) *Quercus/Pinus* (Q/P) rate and *Quercus* pollen percentage records from core CJ06-435, bold-blue and bold-red lines are the five-point running average. As introduced in part 5.4 “Palaeovegetation reconstruction and its climate significance”, there might be some deposition hiatus between 3000 cal. a BP and 1855 AD. So, Q/P rate and *Quercus* pollen percentage records during 3000 cal. a BP and 1855 AD is for reference only. (e) $U^{K_{37}}$ SST record from YS01 core in the south Yellow Sea (Jia et al., 2019). (f) Pollen-based mean annual temperature (MAT) record from Narenxia Peat in the southern Altai (Feng et al., 2017). (g) $U^{K_{37}}$ inferred temperature record at Lake Qinghai (Hou et al., 2016). (h) Pollen-based mean annual temperature record from Lake Bayanchagan in Inner Mongolia, North China (Jiang et al., 2006). (i) Botryococcene concentrations in the El Junco sediment, a proxy for frequency of El Niño events (Zhang et al., 2014). (j) Variance of $\delta^{18}O$ values of individual planktonic foraminifera (*G. ruber*) in sediment core V21–30 from the Galápagos region, a proxy for ENSO variance (Koutavas and Joanides, 2012).

Figure 1



2051
2052
2053
2054
2055

Figure 2

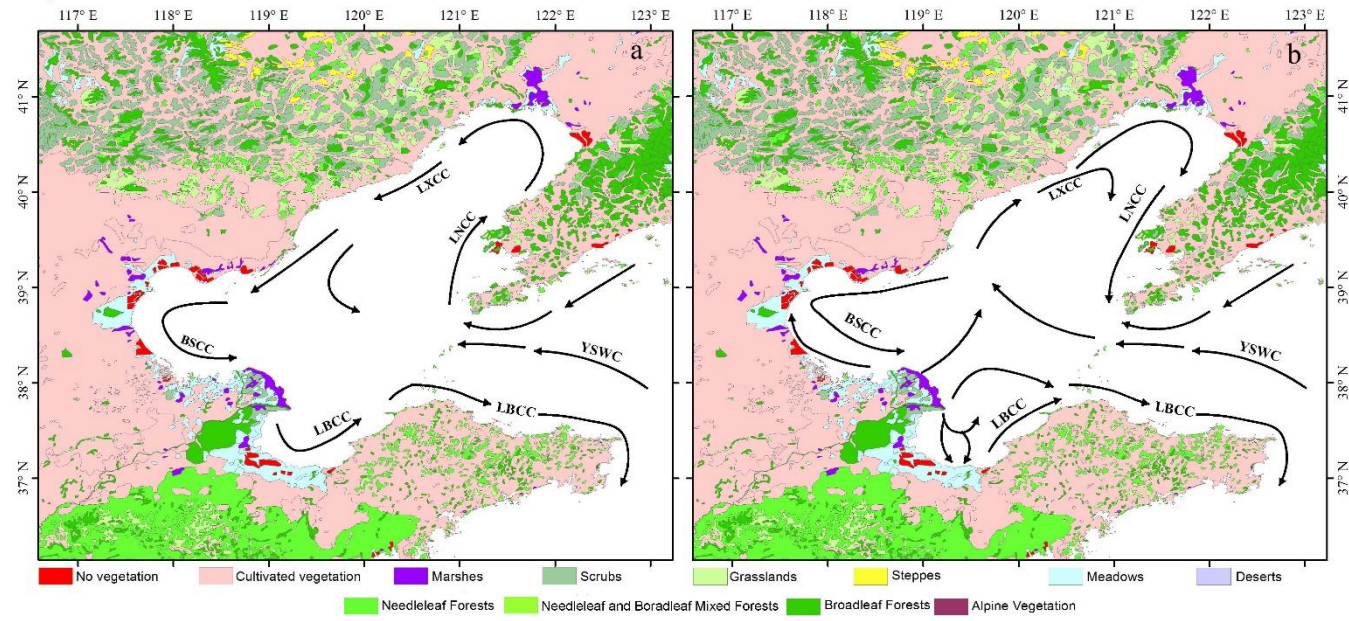


Figure 3

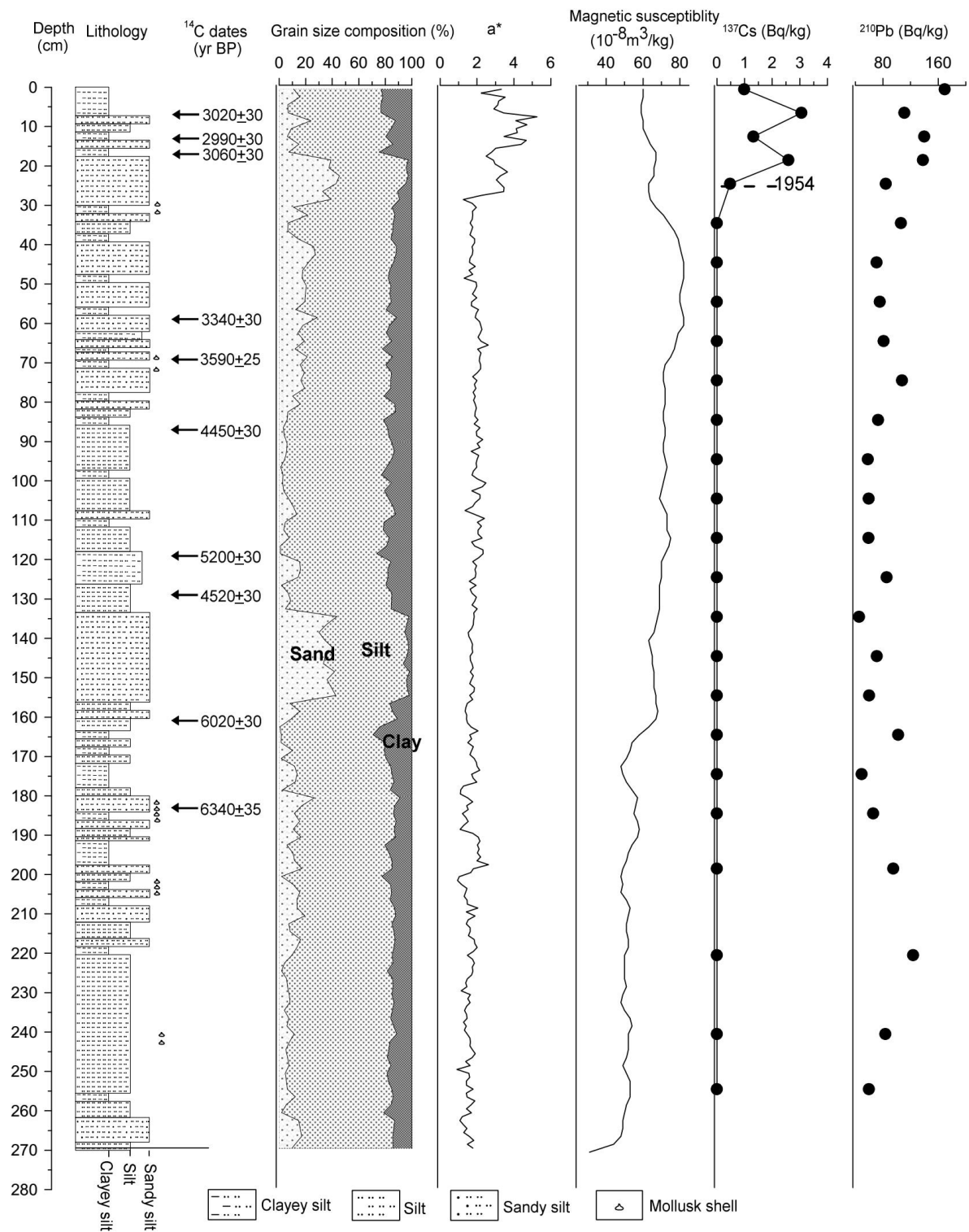


Figure 4

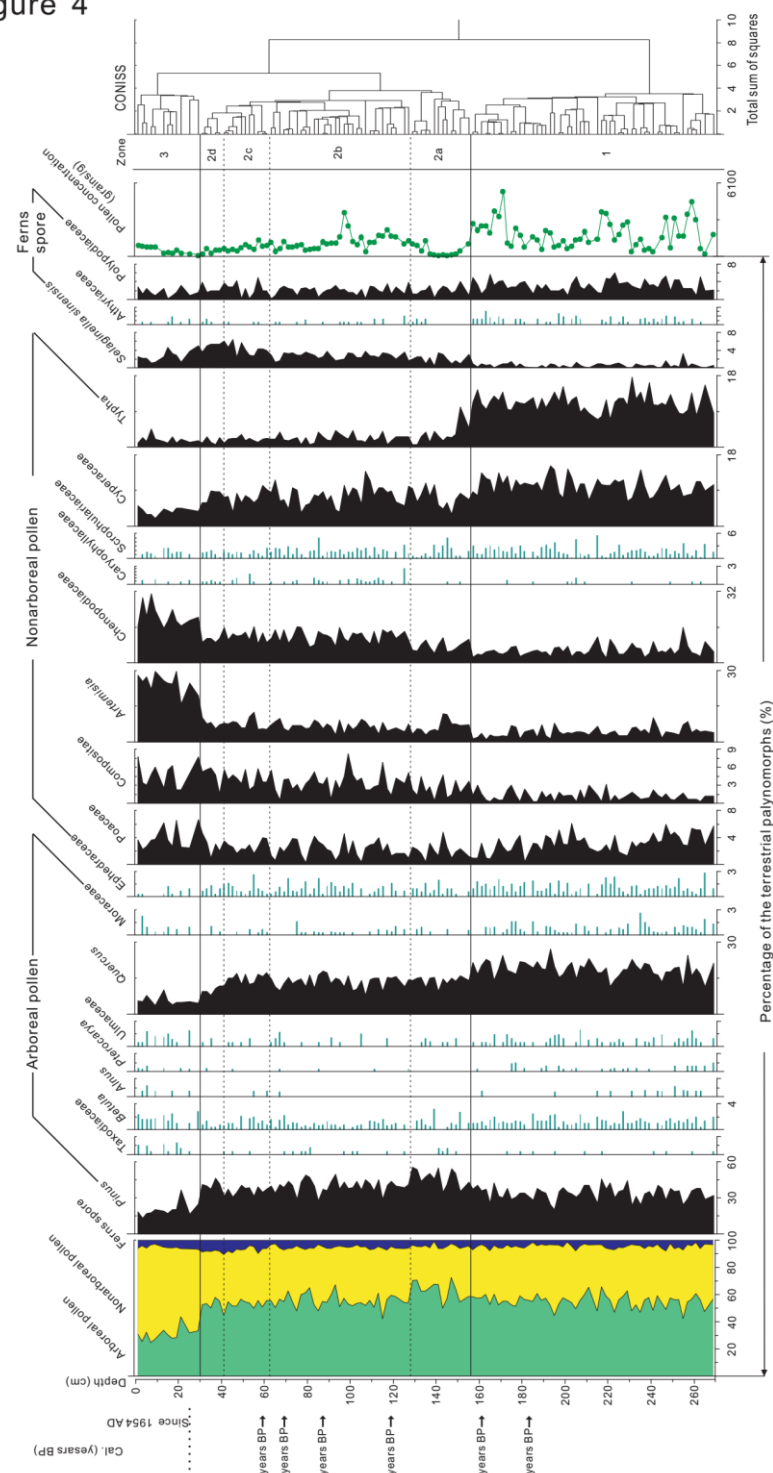


Figure 5

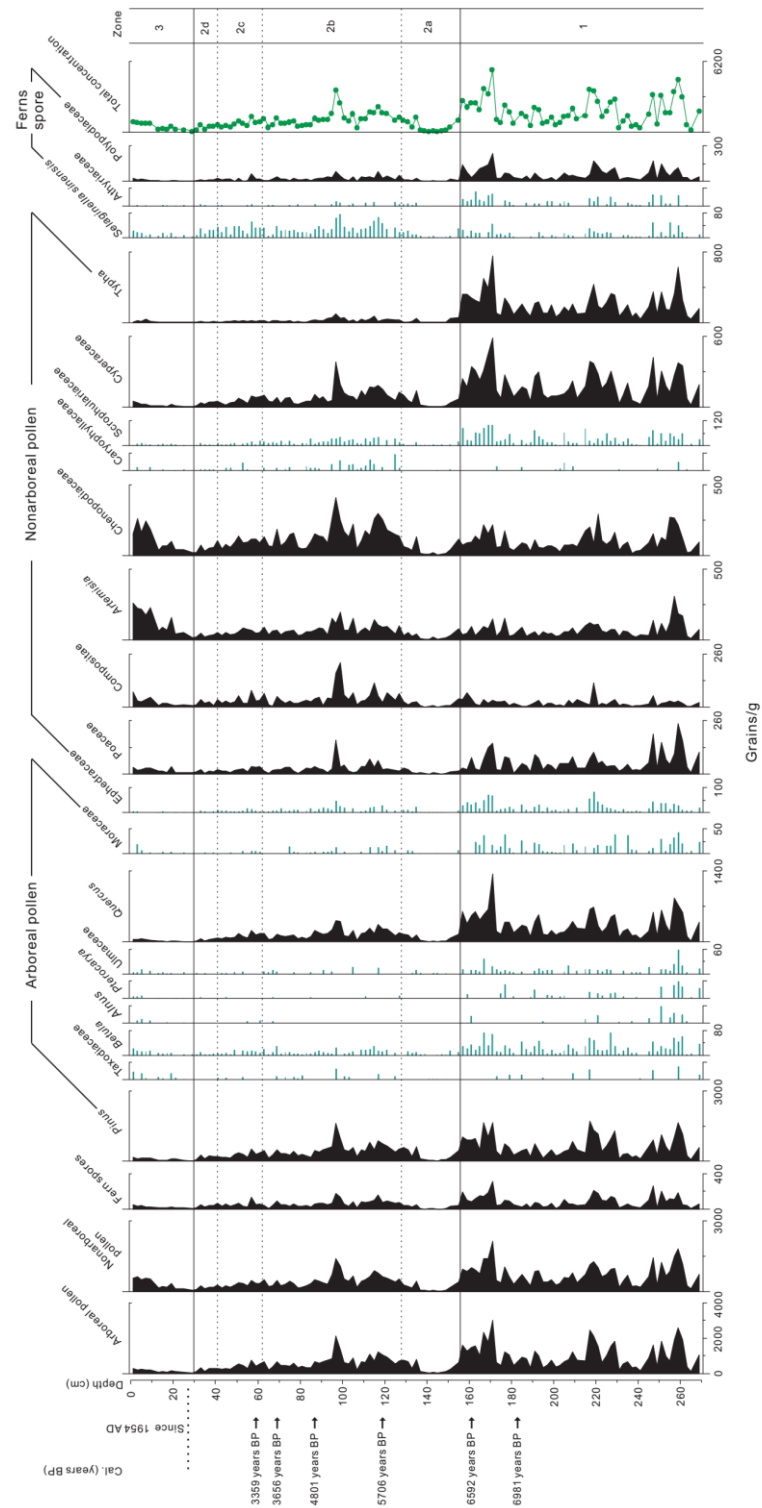
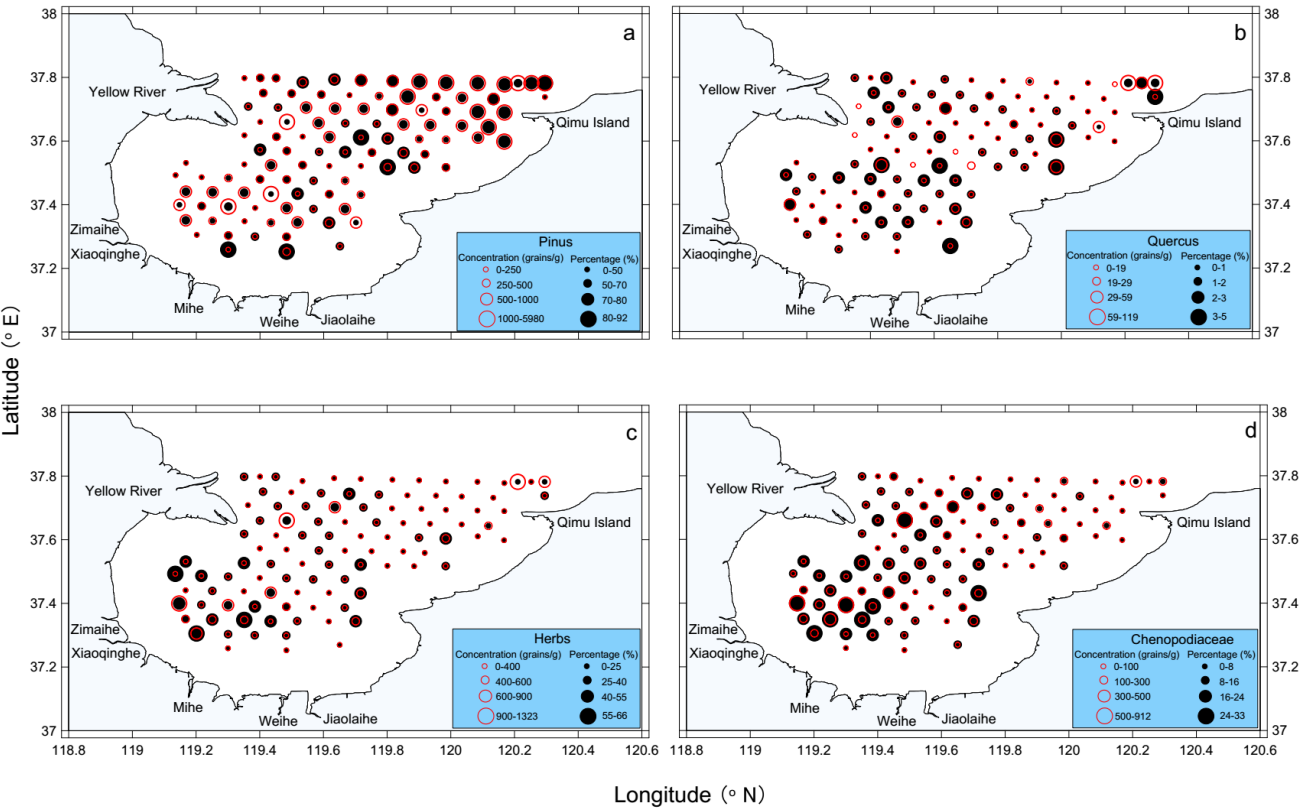


Figure 6



2062

2063

2064

2065

2066

2067

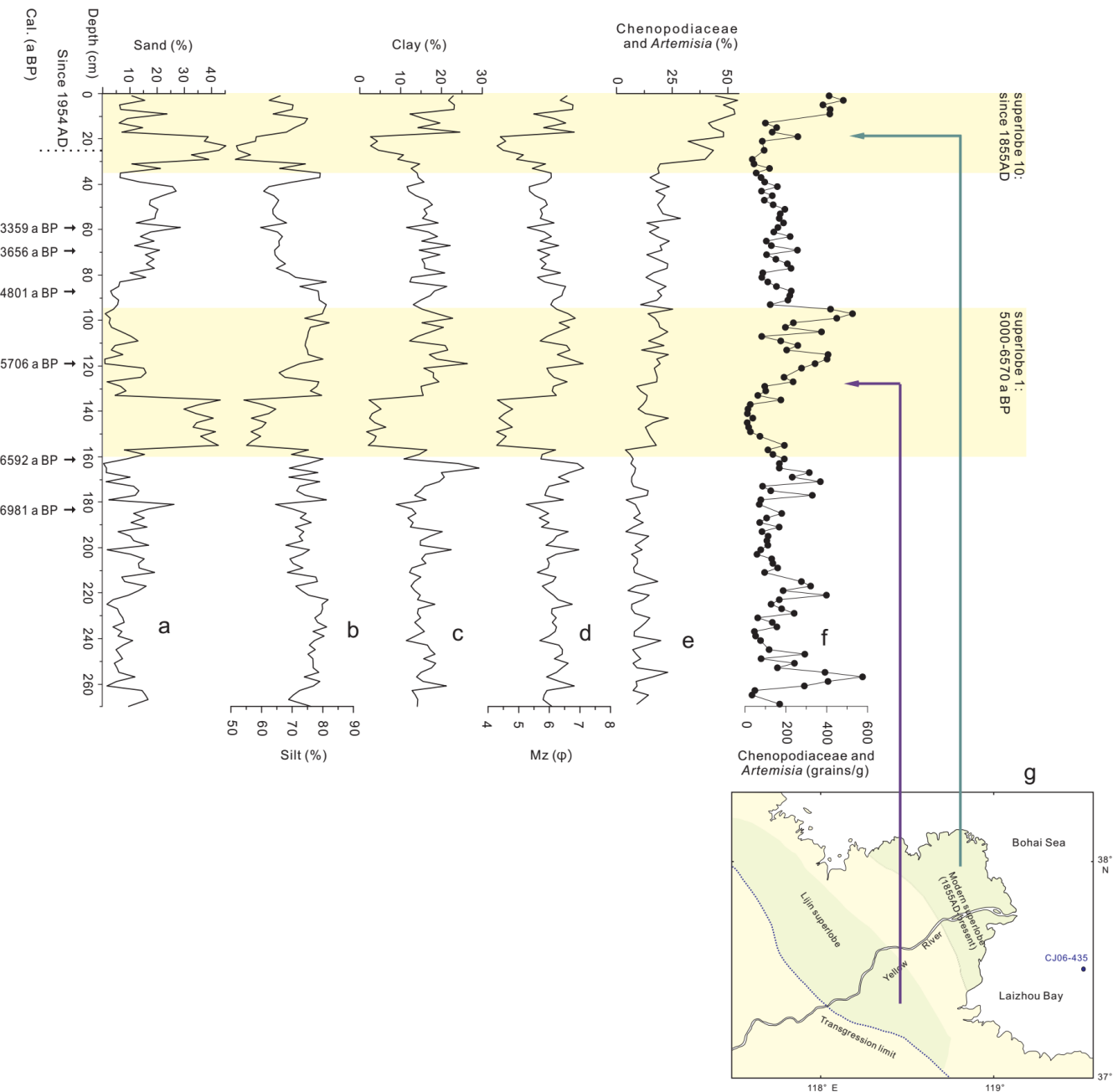
2068

2069

2070

2071

Figure 7



2072

2073

Figure 8

